Envisat GDR
Cross calibration Report

Cycle 041

19-09-2005 24-10-2005

Prepared by :	Y. Faugere, CLS F. Mertz, CLS J. Dorandeu, CLS	
Accepted by :	J. Dorandeu, CLS	
Approved by :	N. Picot, CNES	

SALP-RP-P2-EX-21121-CLS041
Edition 01.0, May 2006

1 Introduction. Document overview

The purpose of this document is to report the major features of the cross-calibration between Envisat and the ERS-2 and Jason-1 missions. The document is associated with data dissemination on a cycle by cycle basis.

The objectives of this document are :

- To present the major useful cross-calibration results for the current cycle
- To report any change likely to impact the comparison between Envisat and other missions, from instrument status to software configuration

It is divided into the following topics:

Cycle overview
Cross Calibration with ERS-2
Cross Calibration with Jason-1

2 Cycle overview

Envisat cycle 041 has been produced with the IPF processing chain V5.02 and the CMA Reference Software V7.1_05. The content of this science software version is described in a document available on the ESA PCS web site ([3]). The Envisat quality assessment report ([4]) summarizes the major features of the Envisat data quality for this cycle of data.

The cross-calibration with ERS-2 OPR2 version 6.5 from CERSAT centre has been performed with ERS-2 OPR cycle 109. The main results for cycle 109 are reported in the ERS-2 Quality assessment report [10]. All the necessary updates were performed on ERS-2 data to be homogeneous with the Envisat data set.

The cross-calibration with Jason-1 GDRs (CMA Reference Software V7.1_04) has been performed with Jason-1 GDRs cycles 136 to 140. The content of this science software version is described by N.Picot (electronic communication, October 21, 2005) [12]). The Jason-1 quality assessment report ([1]) summarizes the major features of the Jason-1 data quality for these cycle of data.

3 Cross Calibration with ERS-2

Envisat flies on the same ground track as ERS-2, about 30 minutes ahead. This section presents results that illustrate the difference with ERS-2.
A failure of the ERS-2 tape recorder occured on 22 June 2003. The ERS-2 Low Rate mission continues within the visibility of ESA ground stations over Europe: North Atlantic, Arctic and western North America. Nevertheless, cross calibration with ERS-2 can be performed on this zone. Envisat cycle 041 data and data from ERS-2 OPR cycle 109 are collocated by repeat-track analysis in order to compare the in order to compare the SWH, backscatter coefficient and radiometer wet troposphere correction.

3.1 Cycle results

3.1.1 [ERS-2 - Envisat] Ku SWH differences

(ERS-2 - Envisat) Ku SWH differences are plotted on the following map (data are centered about the mean value).

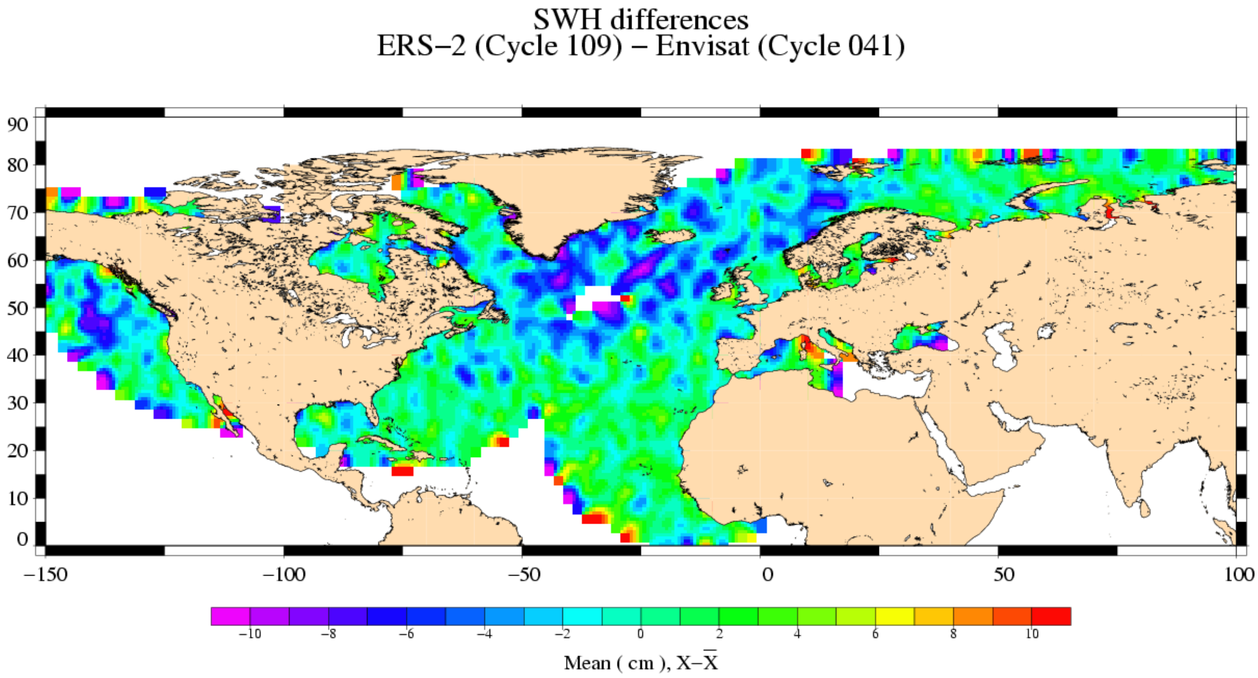

Analysis	Number	Mean (m)	Std. dev. (m)
E2-EN SWH	194756	-0.24	0.27

The Ku SWH values from ERS-2 and Envisat are compared in the next two charts, respectively, the scatter plot between ERS-2 and Envisat SWH values and a plot of (ERS-2 - Envisat) SWH differences as a function of SWH values.

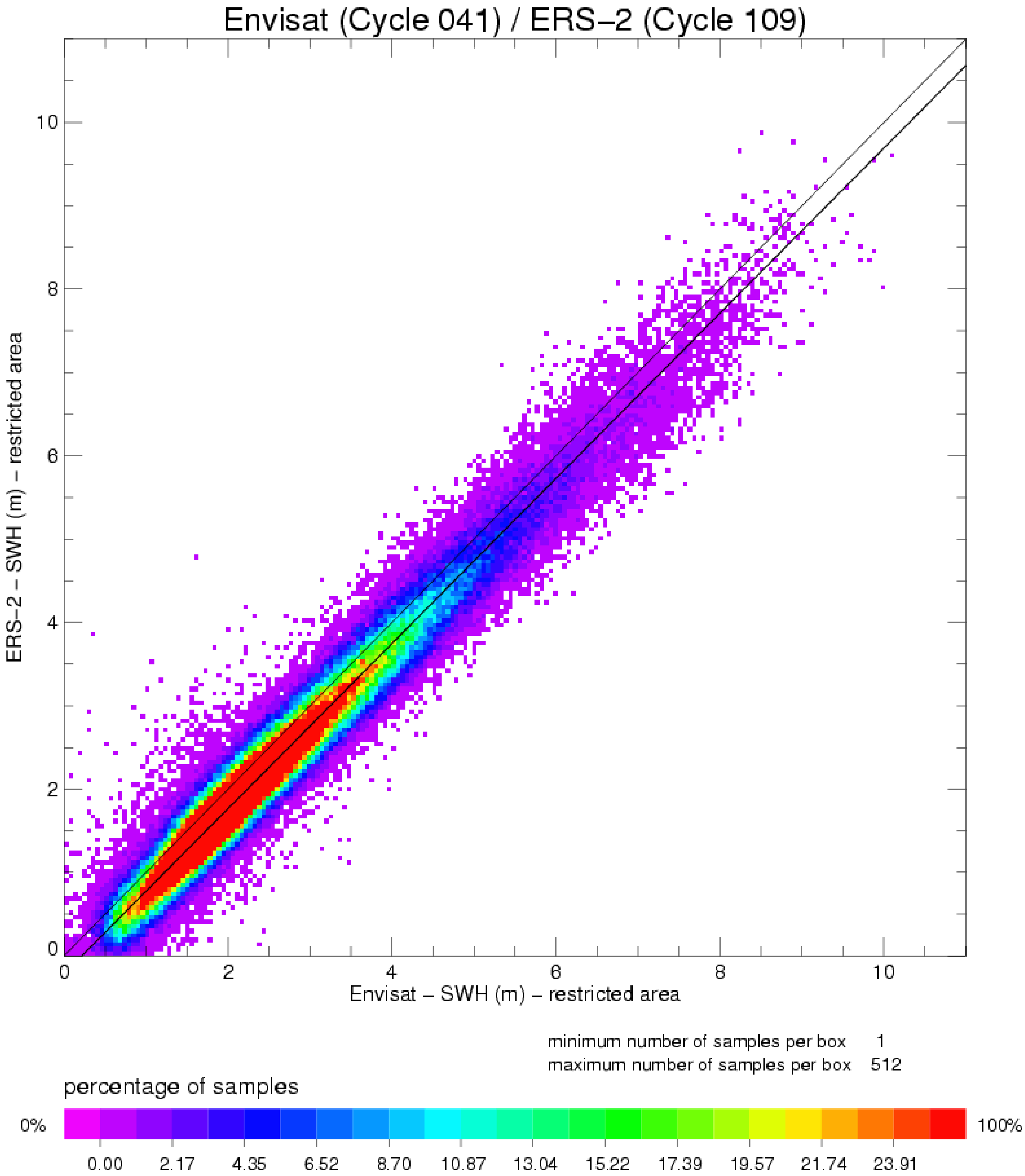

Statistics Y–X

mean = –0.23781
rms = 0.36180
std = 0.27267

Statistics Y,X

samples = 194573
covar = 1.59386
r = 0.97703

Linear regression

type: least rectangle

y = ax + b
a = 0.99080519
b = –0.21553860

Statistics X

mean = 2.55113
rms = 2.85565
std = 1.28315

Statistics Y

mean = 2.31213
rms = 2.63861
std = 1.27135

Legend

—— Linear regression
—— Bisectrix

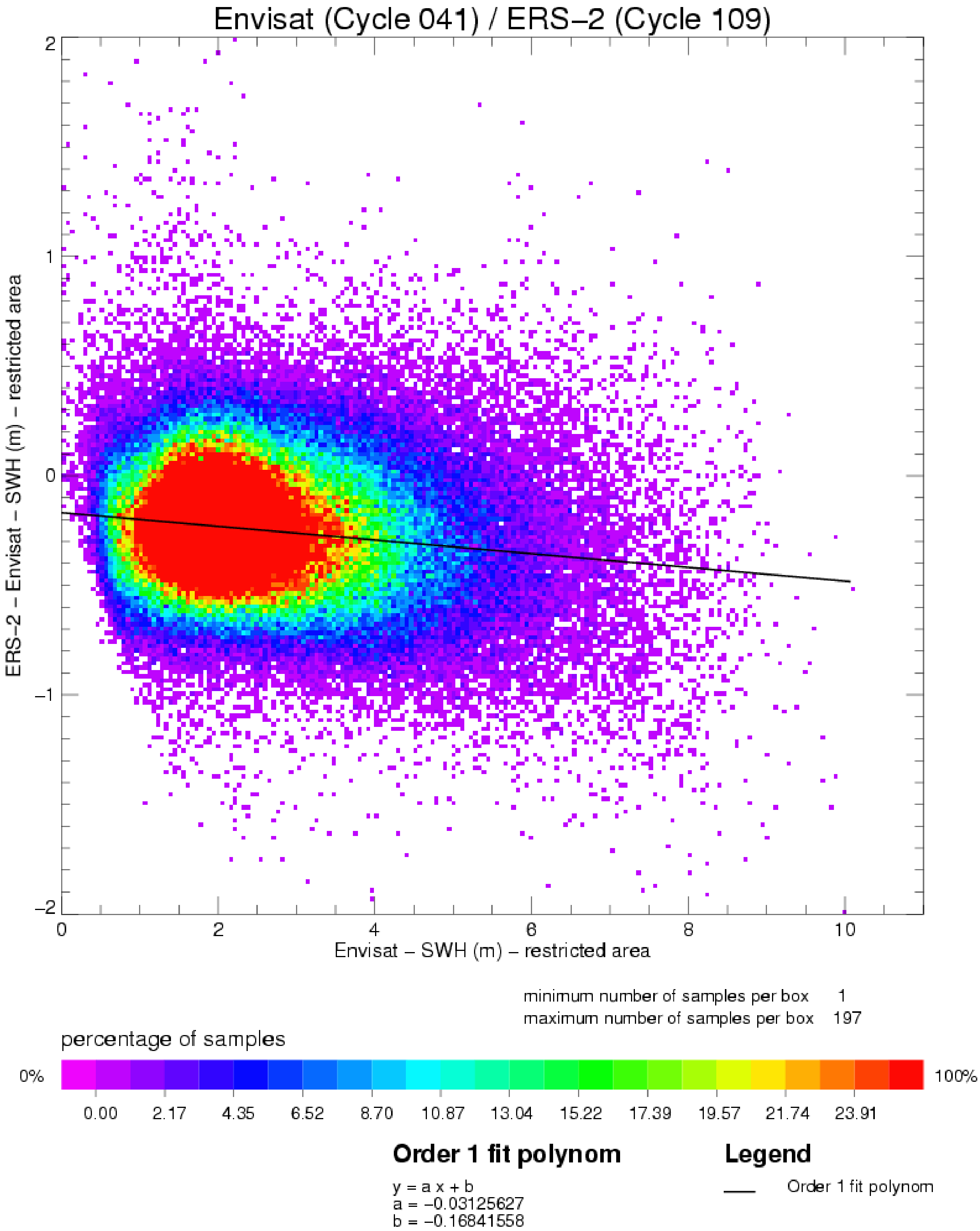
Envisat (Cycle 041) / ERS−2 (Cycle 109)
ERS−2 − Envisat − SWH (m) − restricted area
Envisat − SWH (m) − restricted area
2
1
0
−1
−2
0
2
4
6
8
10
minimum number of samples per box 1
maximum number of samples per box 197
percentage of samples
0%
100%
0.00
2.17
4.35
6.52
8.70
10.87
13.04
15.22
17.39
19.57
21.74
23.91
Order 1 fit polynom
y = a x + b
a = −0.03125627
b = −0.16841558
Legend
Order 1 fit polynom

The cycle by cycle mean ERS-2-Envisat difference of Ku-band SWH is plotted in the following figure:

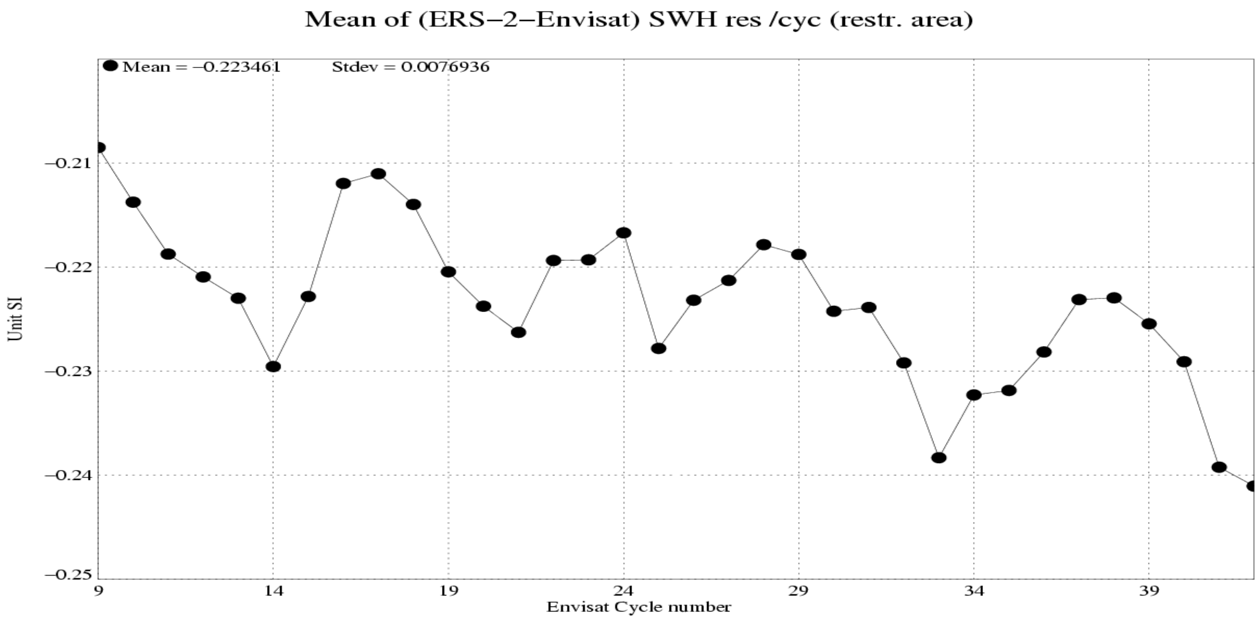

These differences are quite stable. Envisat SWH is 22 cm higher than ERS-2 SWH.

3.1.2 [ERS-2 - Envisat] Ku Sigma0 differences

(ERS-2 - Envisat) Ku SIGMA0 differences are plotted on the following map (data are centered about the mean value).

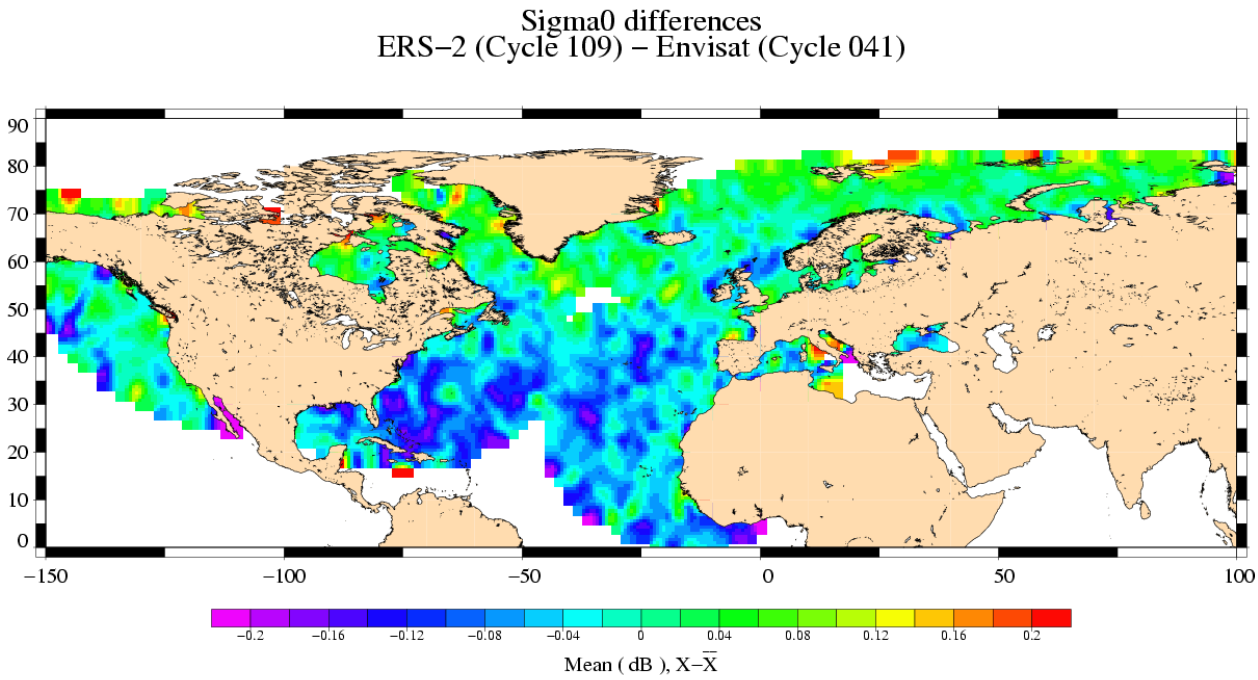

Analysis	Number	Mean (dB)	Std. dev. (dB)
E2-EN Sigma0	194756	0.19	0.28

Wet areas appear because the ERS-2 atmospheric attenuation is uncomplete (it only accounts for cloud liquid water path attenuation), contrary to the Envisat one. Note that the ERS-2 SIGMA0 has been corrected for a bias (+0.25 dB) as described in Dorandeu, 2000 [2].

The Ku SIGMA0 values from ERS-2 and Envisat are compared in the next two charts, respectively, the scatter plot between ERS-2 and Envisat SIGMA0 values and a plot of (ERS-2 - Envisat) SIGMA0 differences as a function of SIGMA0 values.

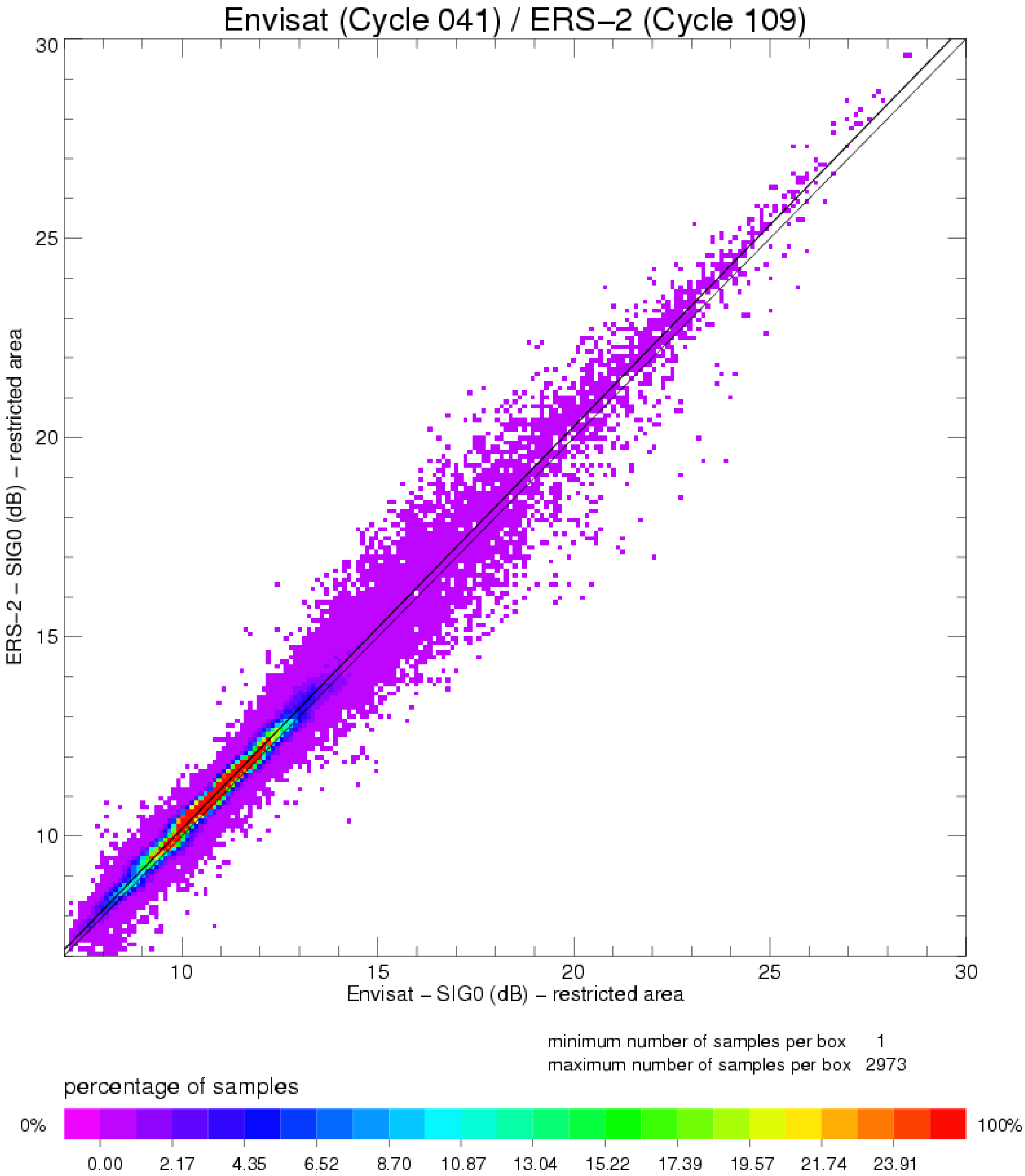

Statistics Y−X

mean = 0.19033
rms = 0.34006
std = 0.28181

Statistics Y,X

samples = 194743
covar = 2.85715
r = 0.98621

Linear regression

type: least rectangle

y = ax + b
a = 1.01020963
b = 0.07903981

Statistics X

mean = 10.99391
rms = 11.12358
std = 1.69347

Statistics Y

mean = 11.18520
rms = 11.31527
std = 1.71076

Legend

—— Linear regression
—— Bisectrix

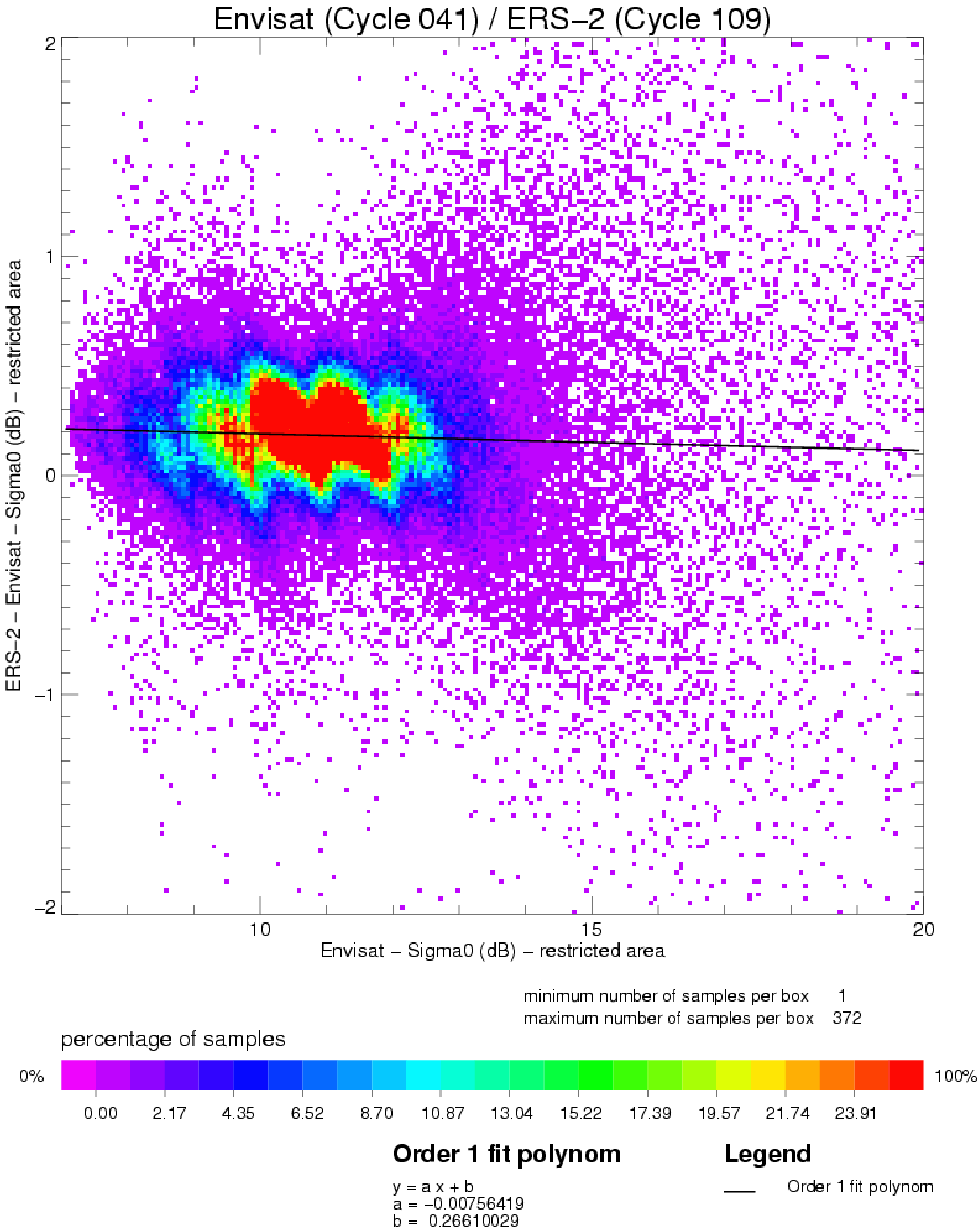

The particular features of the SIGMA0 differences mainly come from the shape of the ERS-2 histogram.

The cycle by cycle mean ERS-2-Envisat difference of Ku-band Sigma0 is plotted in the following figure:

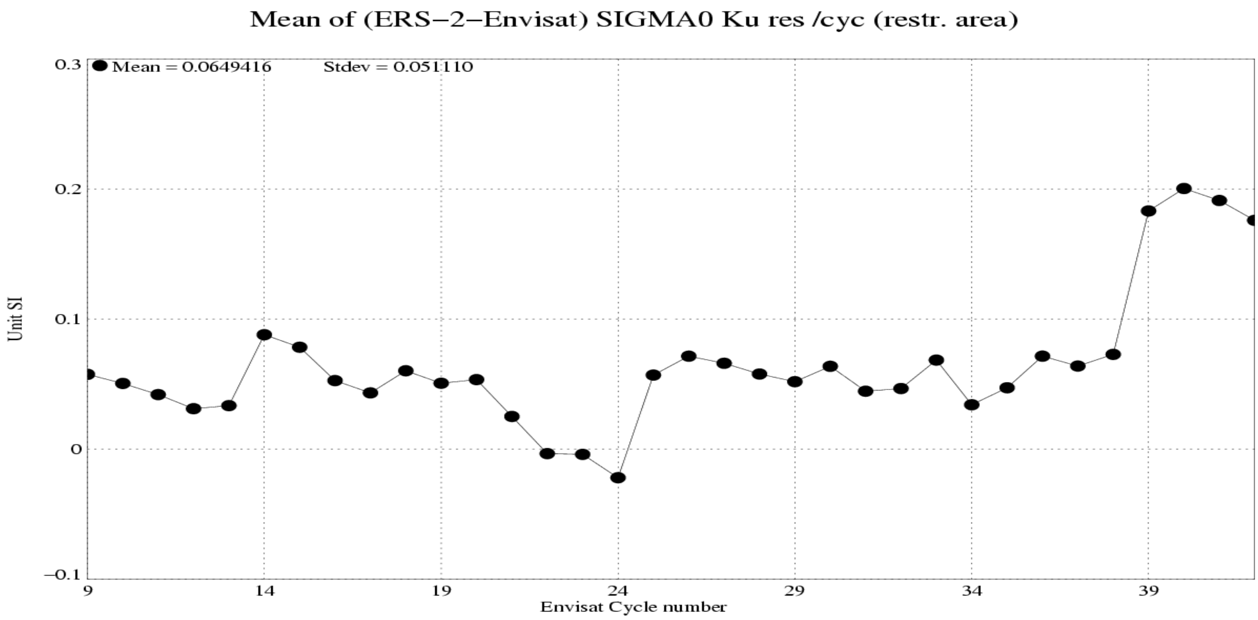

The mean ERS-2-Envisat Ku-band Sigma0 difference is between 0 and 0.1 dB for cycles 9-38. However, this mean value accounts for the calibration correction applied in the ground processing to enter the wind speed algorithm. The monitoring of (ERS-2 - Envisat) Sigma0 differences exhibits a 0.1 dB jump between cycles 38 and 39. This jump occurs at the end of cycle 38, on the 4th July 2005 11:29 UTC. Since no jump is observed on the Envisat/Jason-1 differences, it may be attributed to ERS-2.

3.1.3 [ERS-2 - Envisat] radiometer wet troposphere correction differences

The ERS-2 radiometer correction is recomputed to correct for the gain drop and for the drift of the 24 GHz brightness temperature (Obligis et al., 2003 [11]).

(ERS-2 - Envisat) Radiometer wet troposphere correction differences are plotted on the following map (data are centered about the mean value).

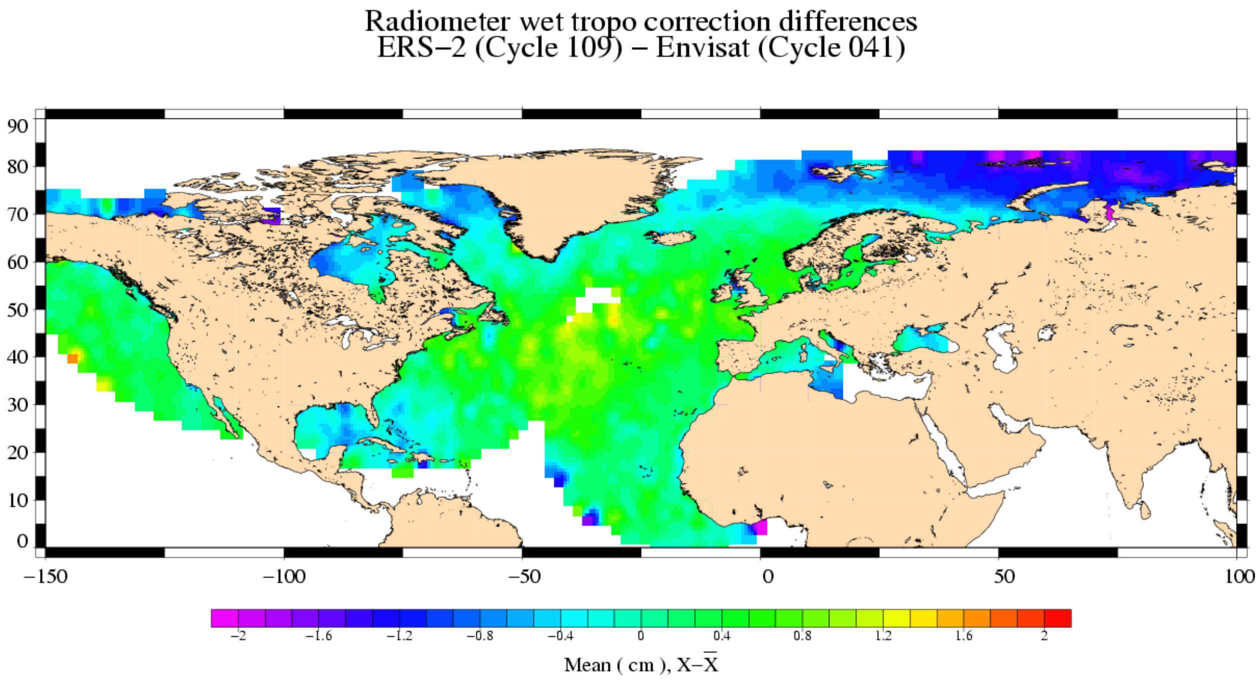

Analysis	Number	Mean (cm)	Std. dev. (cm)
E2-EN radiometer	194756	-0.74	1.00

The MWR wet troposphere corrections from ERS-2 and Envisat are compared in the next two charts, respectively, the scatter plot between ERS-2 and Envisat values and a plot of (ERS-2 - Envisat) differences as a function of MWR wet troposphere values.

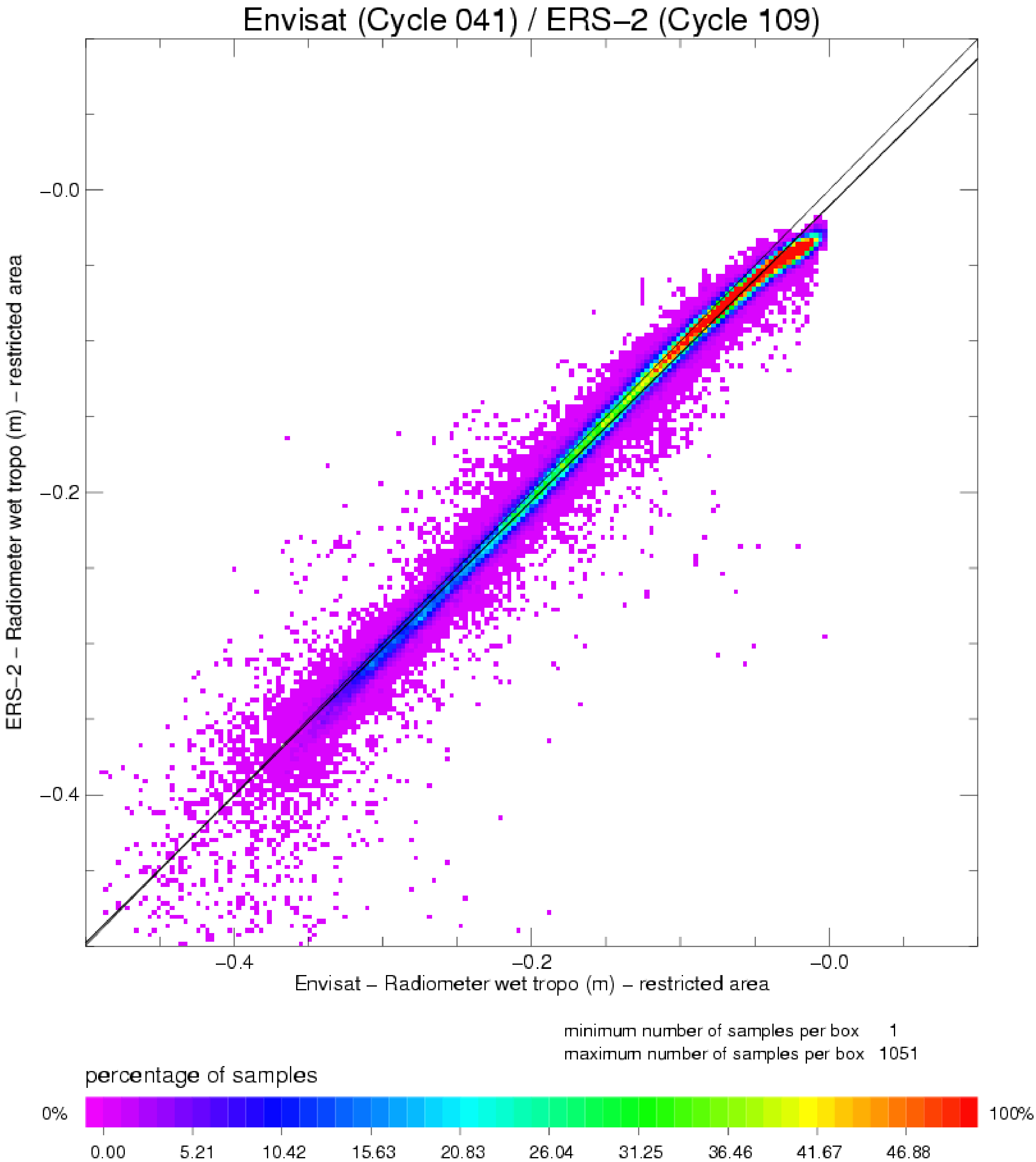

Statistics Y−X

mean = −0.00735
rms = 0.01244
std = 0.01004

Statistics Y,X

samples = 194753
covar = 0.00777
r = 0.99380

Linear regression
type: least rectangle

y = ax + b
a = 0.97519497
b = −0.01057917

Statistics X

mean = −0.12877
rms = 0.15684
std = 0.08954

Statistics Y

mean = −0.13616
rms = 0.16175
std = 0.08731

Legend

—— Linear regression
—— Bisectrix

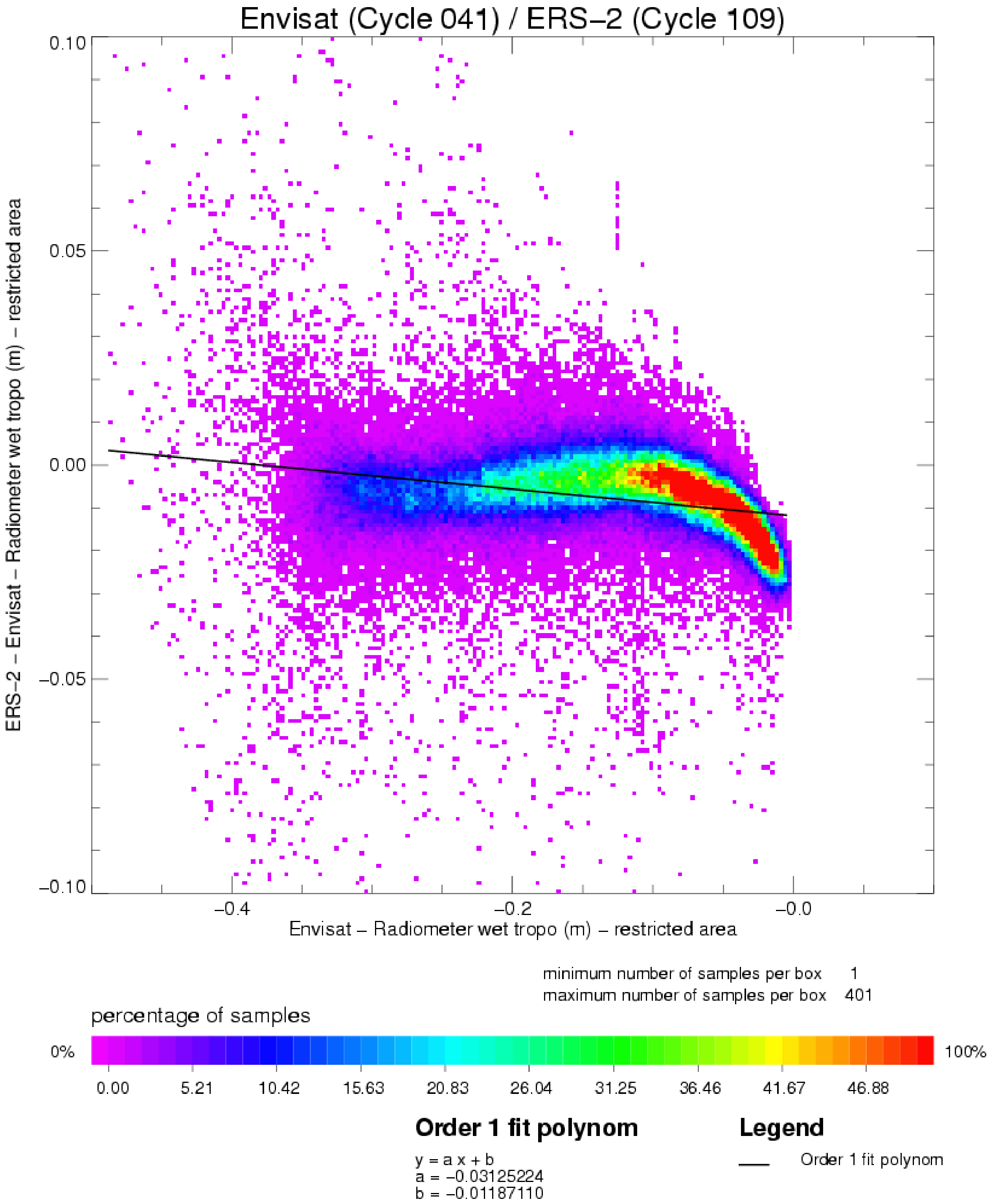

Note that the differences observed in dry conditions are mainly due to the ERS-2 algorithm. Indeed the next scatter plot shows the neural network ERS-2 MWR correction ([6]) and the Envisat one agree very well.

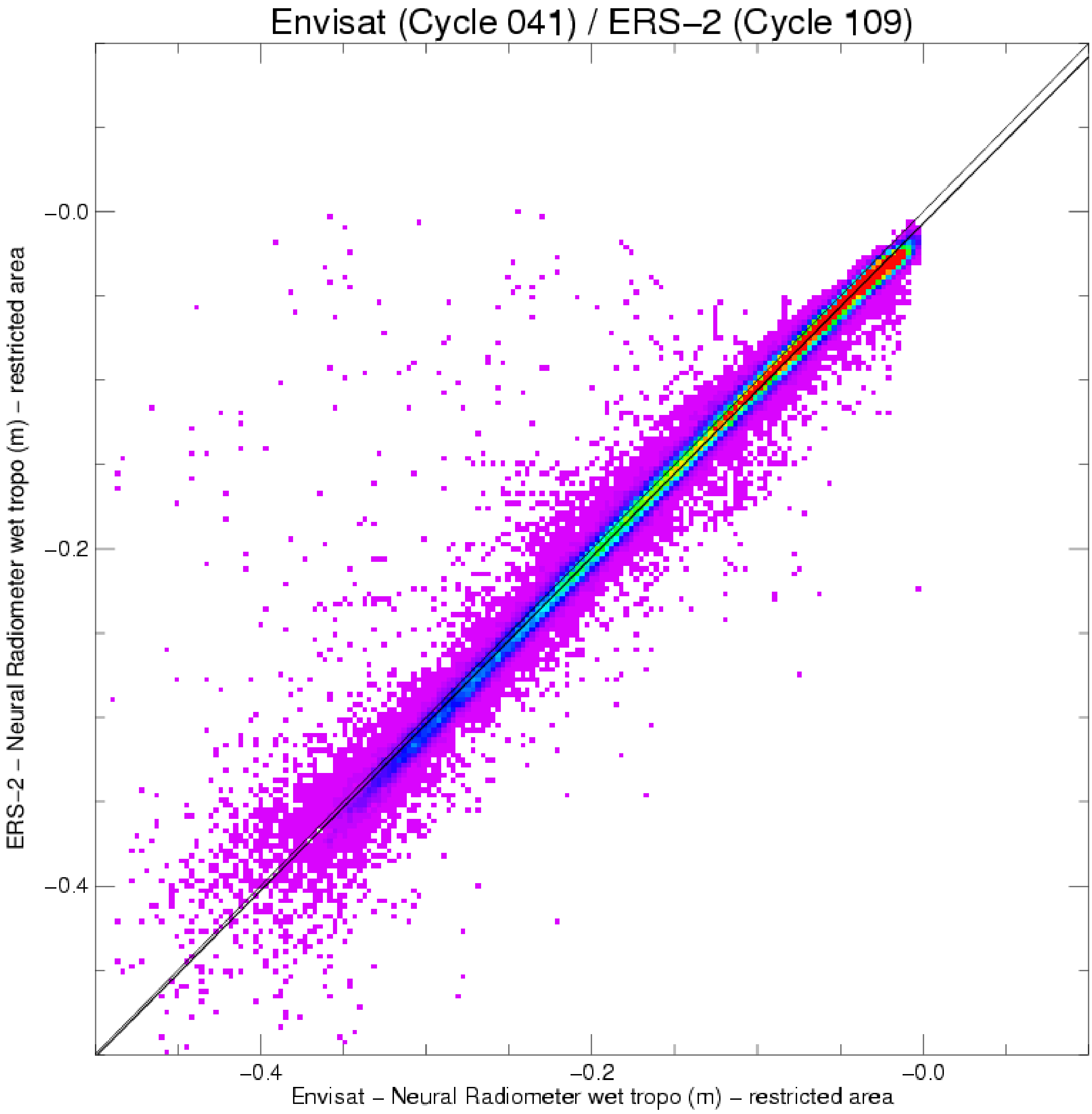

minimum number of samples per box 1
maximum number of samples per box 1052

percentage of samples

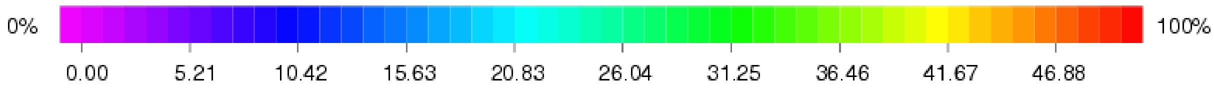

Statistics Y−X

mean = −0.00553
rms = 0.01143
std = 0.01000

Statistics Y,X

samples = 194756
covar = 0.00788
r = 0.99369

Linear regression

type: least rectangle

y = ax + b
a = 0.98963346
b = −0.00689011

Statistics X

mean = −0.12878
rms = 0.15685
std = 0.08954

Statistics Y

mean = −0.13433
rms = 0.16093
std = 0.08861

Legend

Linear regression
Bisectrix

The cycle by cycle mean ERS-2-Envisat difference of the 23.8 GHz brightness temperature, the 36.5 GHz brightness temperature and the wet troposphere correction are plotted in the following figure:

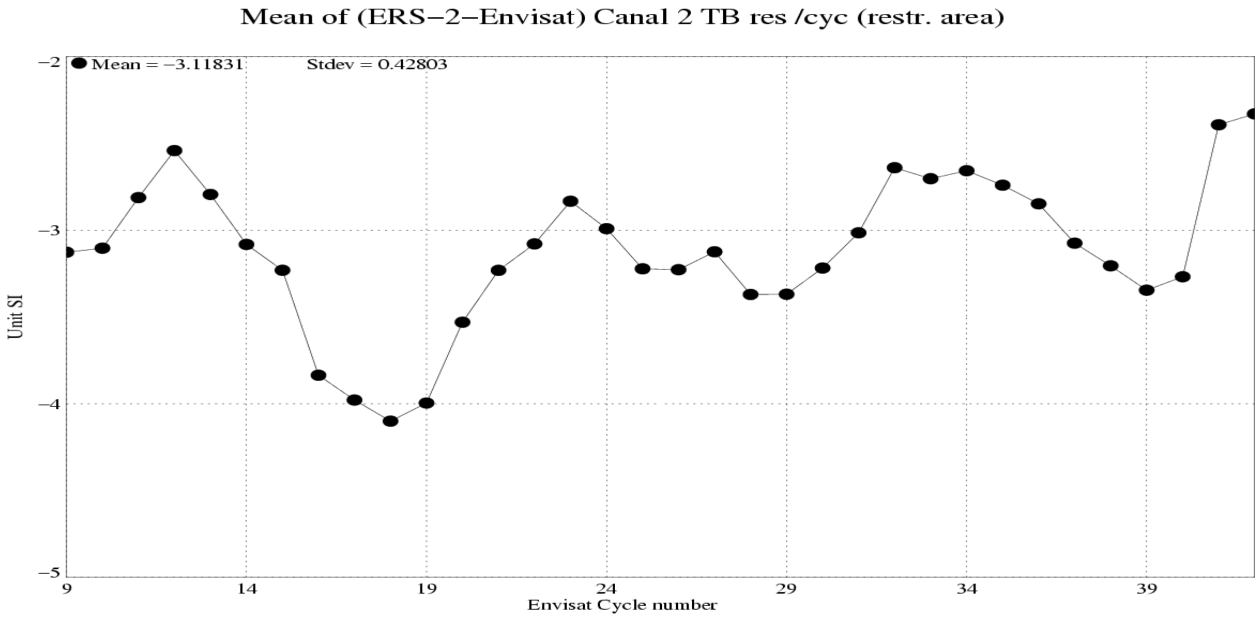

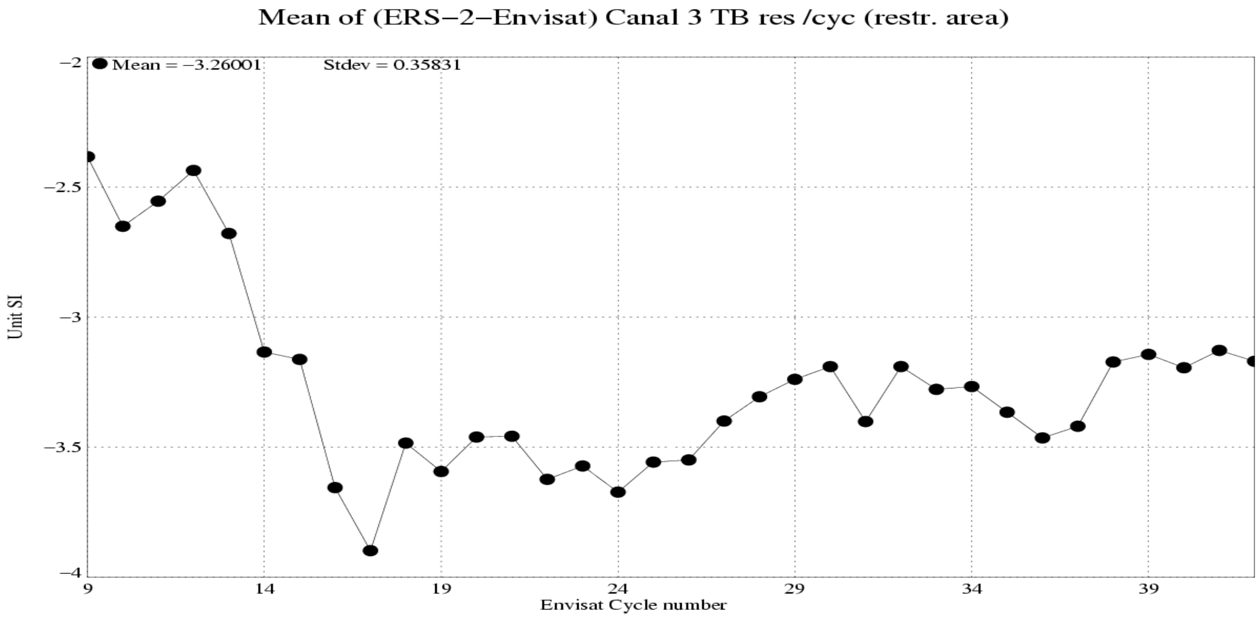

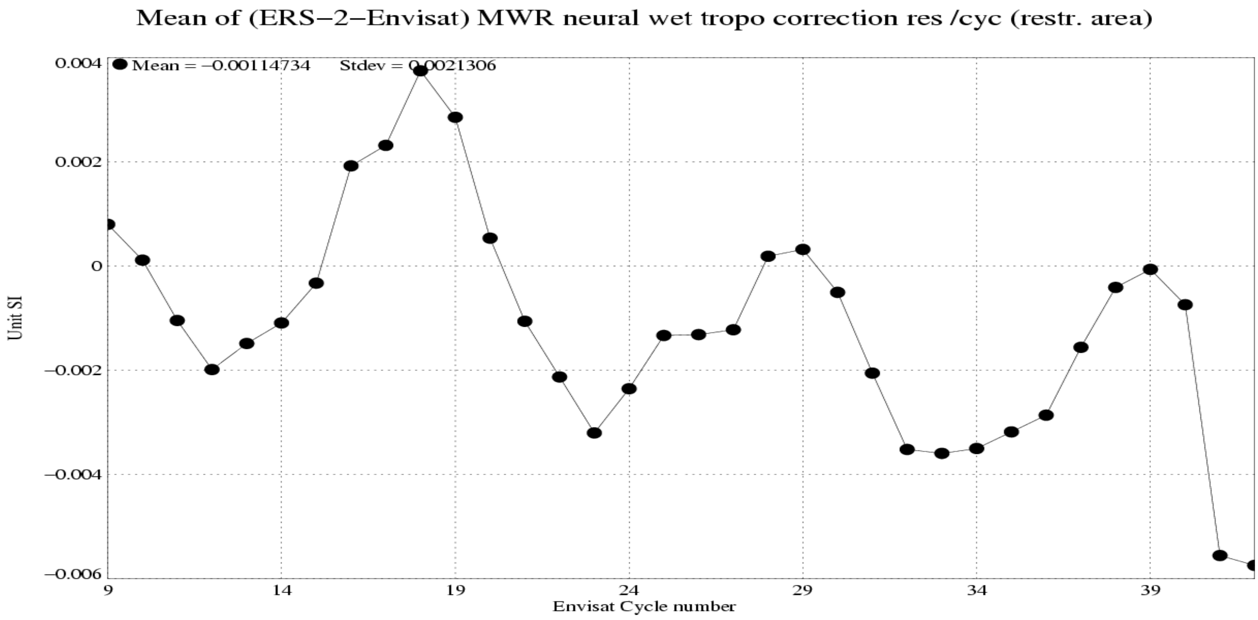

Since the beginning of the mission, the instrumental parameters at 36.5 GHz have been drifting and investigations are in progress to identify the source for these drifts. The impact of this drift is visible on (ERS-2 -Envisat) wet troposphere correction differences.

4 Cross Calibration with Jason-1

Jason-1 GDRs data (cycle 136 to 140) are used for this cross calibration The parameters used to compute the sea surface height (SSH) for Envisat and Jason-1 are:
- Ku range (ocean retracking)
- POE orbit
- Dual frequency ionospheric correction
- MWR derived wet troposphere correction
- ECMWF dry tropospheric correction
- Non parametric sea state bias
- MOG2D
- Total geocentric GOT00 ocean tide height
- Geocentric pole tide height
- Solid earth tide height

Note that within the IPF version 5.02, the actual value of Ultra Stable Oscillator clock period is used within the L1b processing instead of the nominal one as it was used in previous IPF versions. This evolution implies a +2.5 cm jump on the Envisat SSH between cycle 40 and 41. To avoid this jump, and correct for the USO drift, users are advised to apply the correction provided by ESA on cycles 9 to 40 ([9]).

Some comparisons were also performed using the ECMWF wet troposphere correction for both Envisat and Jason-1, to prevent possible discrepancies from radiometer corrections.

Several analyses were performed for this cross calibration study:
- comparison of altimeter and radiometer parameters
- comparison of Sea Level Anomalies relative to a Mean Sea Surface
- computation of a long wavelength error on Envisat
- comparison on a same time/space sampling

10 day crossovers are used to compare SSH estimations from Envisat and Jason-1 while shorter time lags (3 hours) are selected for altimeter and radiometer parameters.

4.1 Dual-crossover points

4.1.1 3-hour and 10-day crossover points location

For Envisat Cycle 041 the location of crossover points with 3-hour and 10 day time lags between Envisat and Jason-1 are given on the following figures:

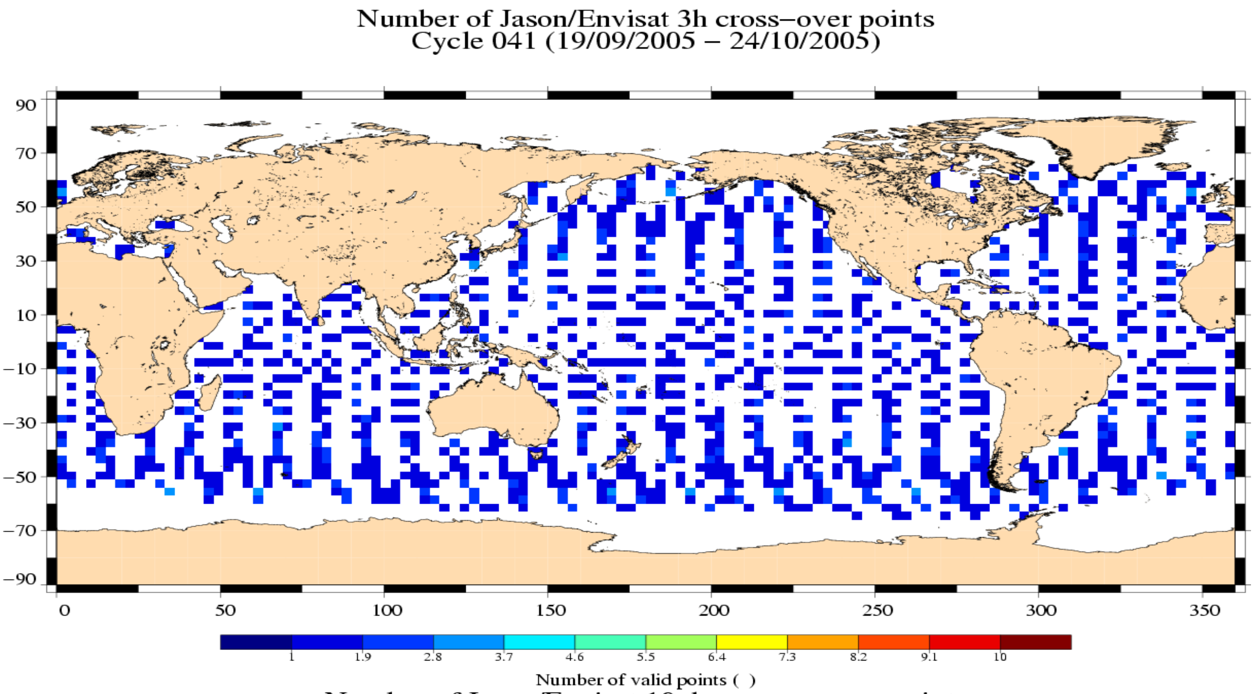

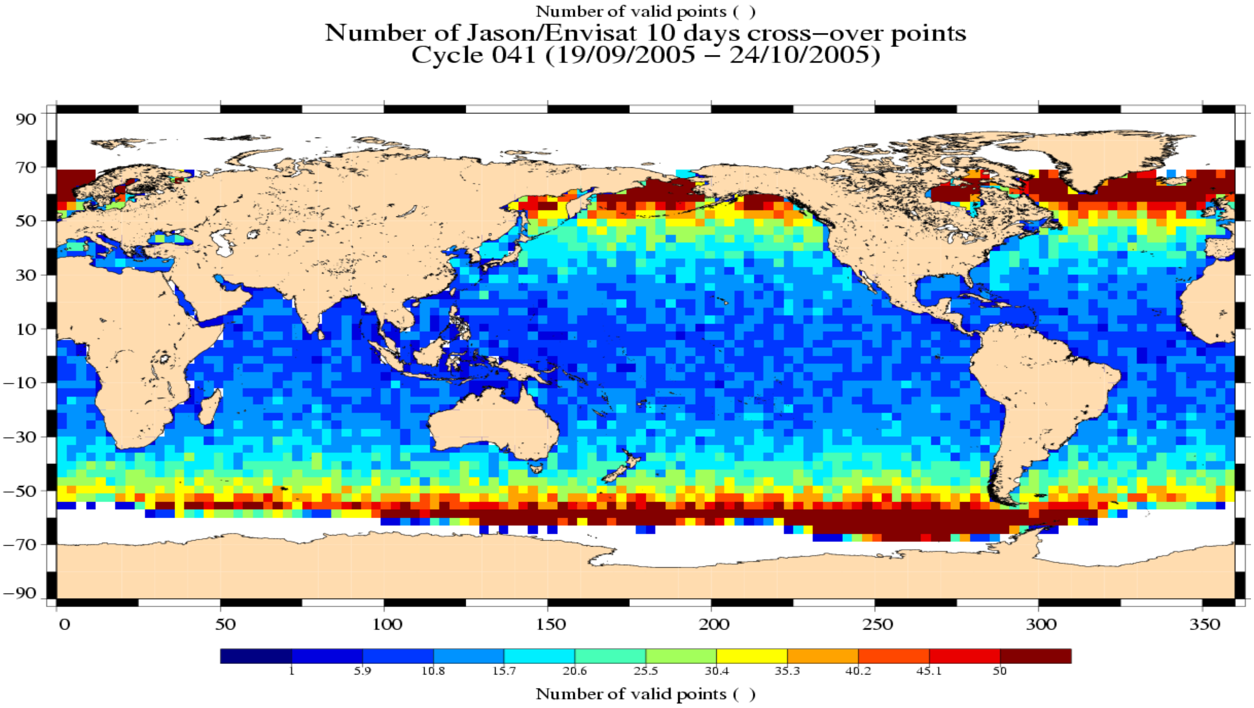

Most of the crossover points are located at high latitude. With 3-hour time lag there are only a few crossover points at mid and low latitudes. This geographical pattern is not constant for every Envisat cycle since Jason-1 is not sun-synchronous. When more Envisat data become available, (Jason-1/Envisat) comparisons will be performed over 12 Jason-1 cycle windows, so that the geographical sampling by Jason-1/Envisat crossovers will be constant.

4.1.2 [Envisat - Jason-1] Ku-band SWH differences

The scatter plot of crossover points with 3-hour time lag between Envisat and Jason-1 Ku-band SWH measurements is given on the following figure:

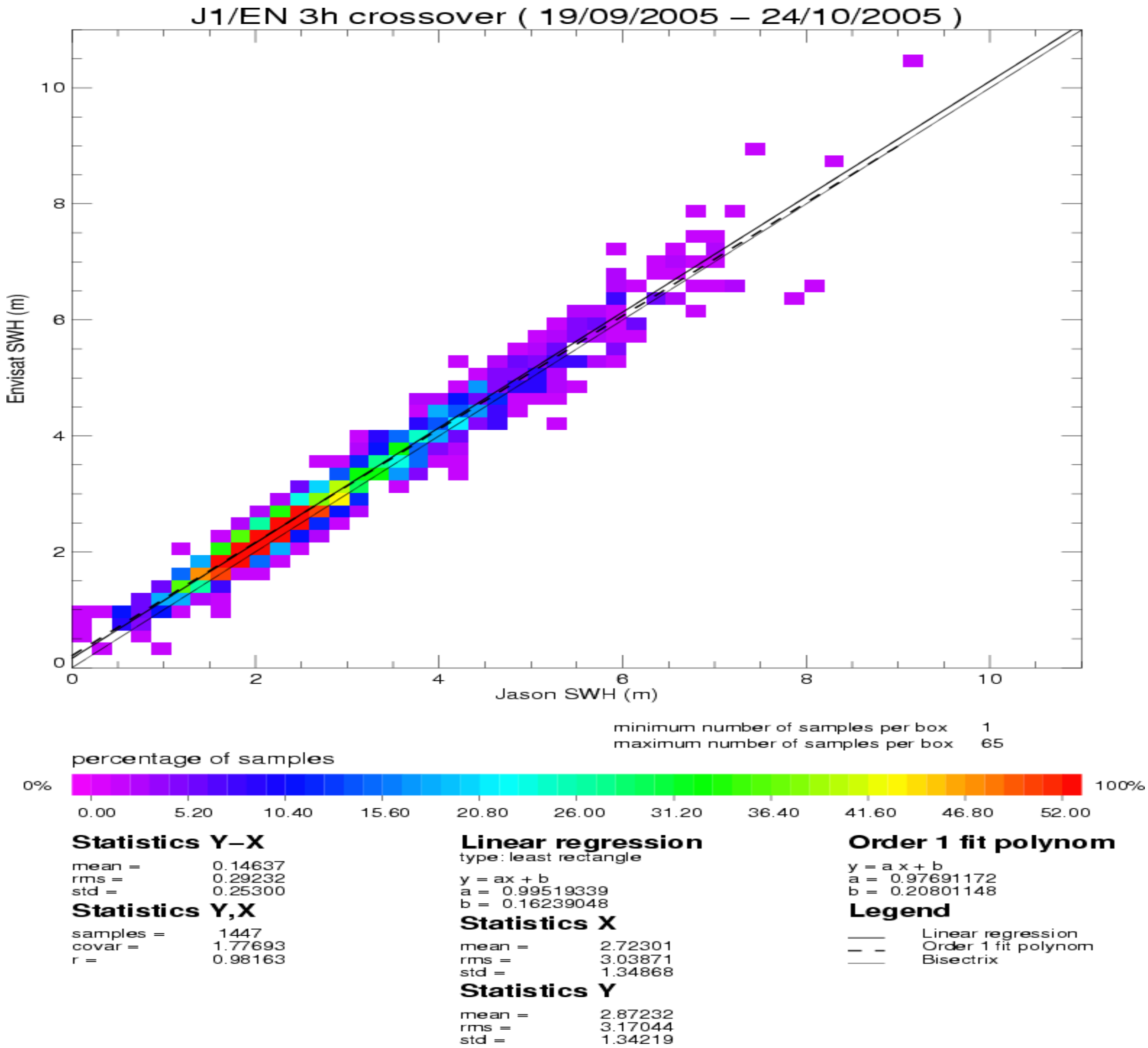

Analysis	Number	Mean (m)	Std. dev. (m)
EN-J1 SWH (m)	1447	0.15	0.24

There is a small bias between the two satellites: Envisat waves are slightly higher than Jason-1 ones.

4.1.3 [Envisat - Jason-1] Ku-band Sigma0 differences

The scatter plot of crossover points with 3-hour time lag between Envisat and Jason-1 Ku-band Sigma0 measurements is given on the following figure:

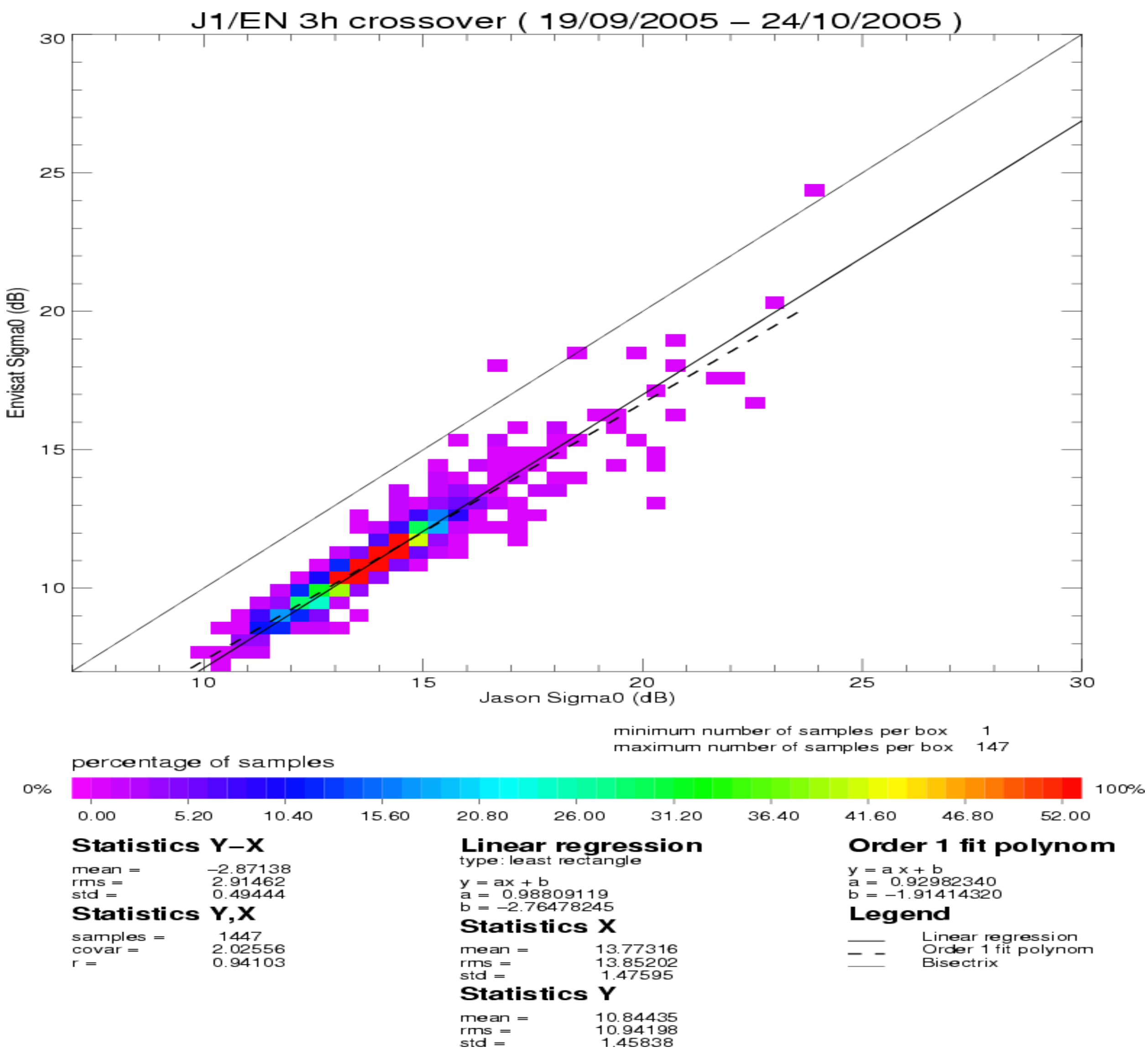

Analysis	Number	Mean (dB)	Std. dev. (dB)
EN-J1 Sigma0 (dB)	1447	-2.93	0.46

Jason-1 Ku-band sigma0 is 2.8 dB higher than Envisat. Envisat Ku-band sigma0 has been aligned on ERS-2 to satisfy the MWC wind model. Notice that Jason-1 Ku-band sigma0 is 2.3 dB higher than TOPEX. This difference is described in (Vincent et al., 2003 [14]).

4.1.4 [Envisat - Jason-1] radiometer wet troposphere differences

The scatter plot of crossover points with 3-hour time lag between Envisat and Jason-1 radiometer wet troposphere correction is given on the following figure:

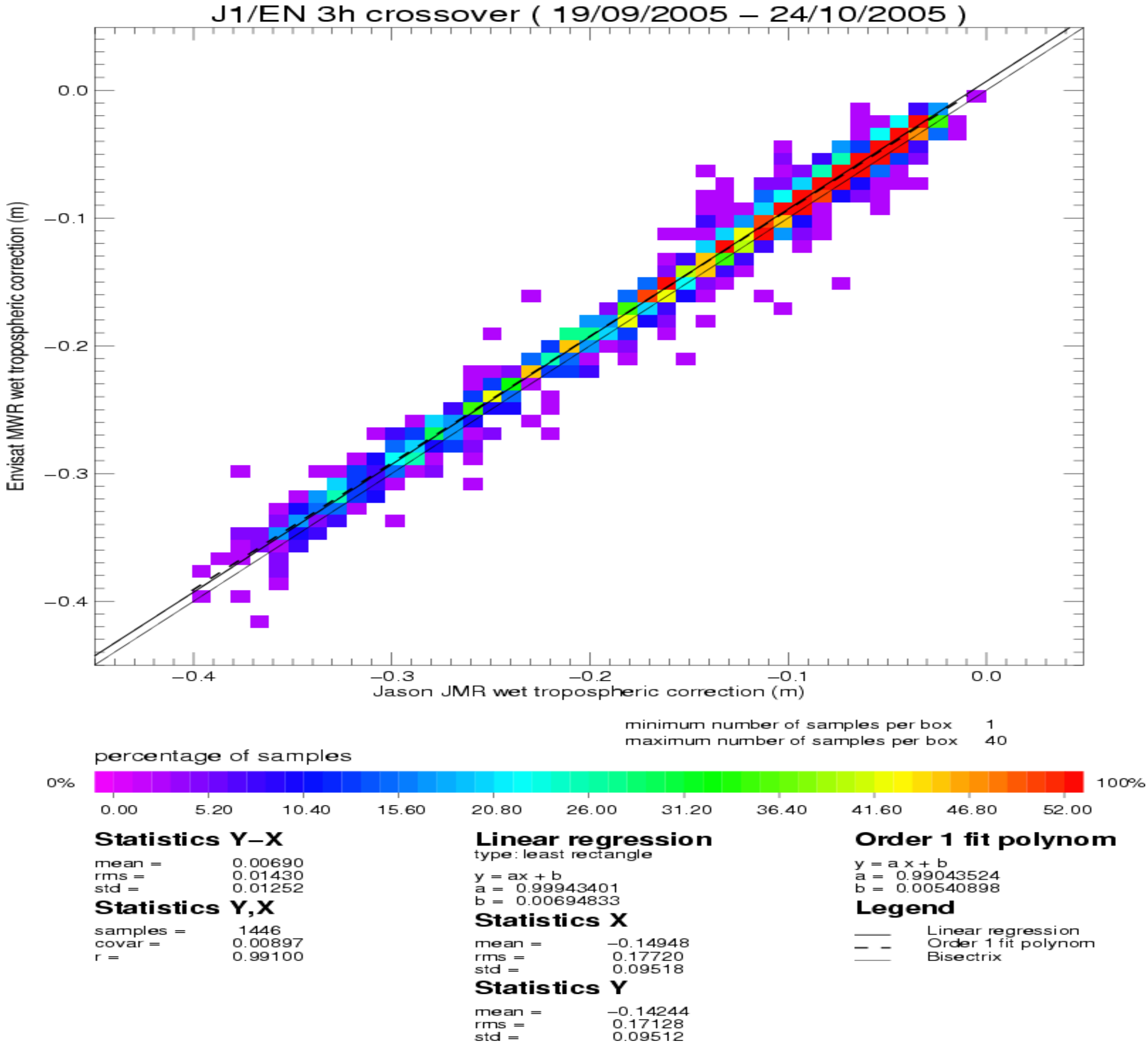

Analysis	Number	Mean (cm)	Std. dev. (cm)
EN-J1 radiometer wet troposphere correction (m)	1447	0.70	1.25

Results are consistent over dry areas. There are not enougth crossover points at low latitudes to comment the differences in wet areas.

4.1.5 [Envisat - Jason-1] SSH differences

[Envisat - Jason-1] SSH differences at crossover points with 10 day time lag are computed in two configurations:
- using the radiometer wet troposphere correction
- using the ECMWF wet troposphere correction

When using a selection to remove shallow waters (1000 m), global statistics are:

Analysis	Number	Mean (cm)	Std. dev. (cm)
EN-J1 SSH	69752	30.03	6.84
EN-J1 SSH with ECMWF wet troposphere	69752	30.74	6.91

The differences are plotted on the following figure (data are centered about the mean value):

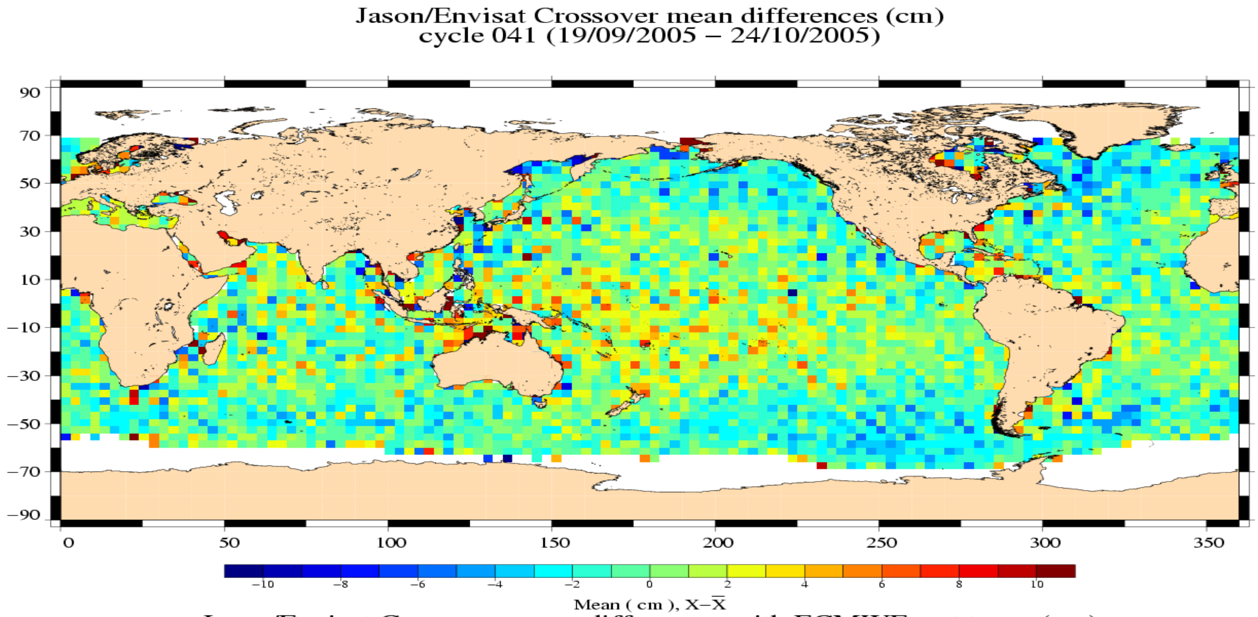

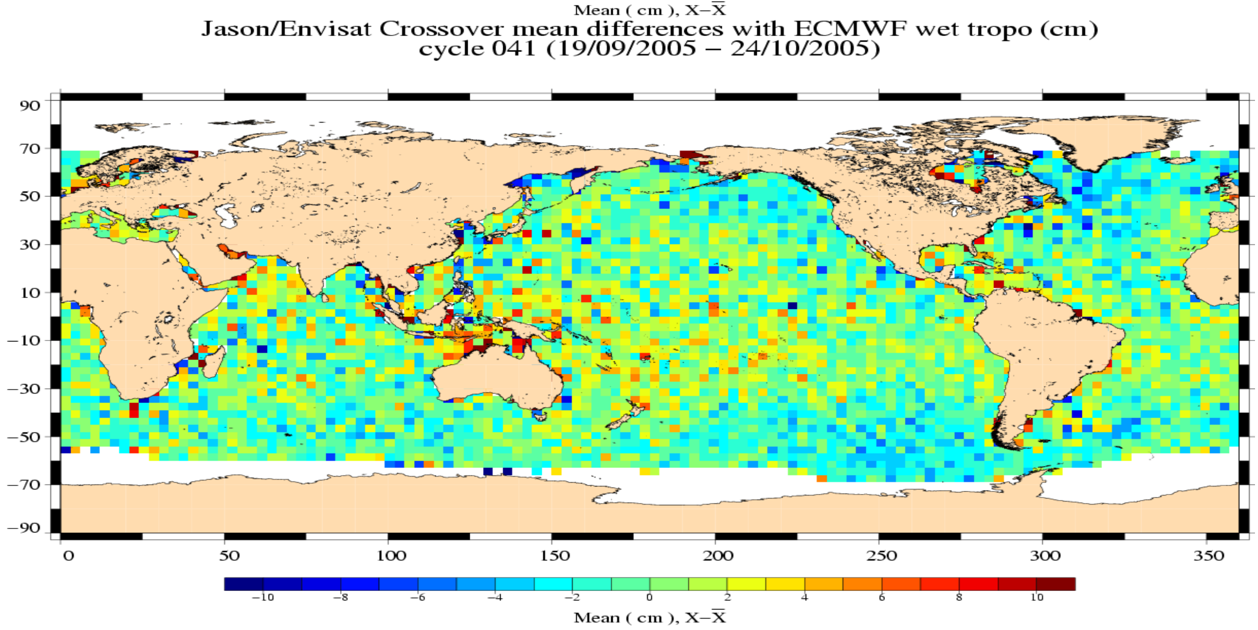

The two maps are very close. There are small scale [Envisat - Jason-1] differences in high variability areas, but also large scale differences in the Pacific ocean.

The cycle by cycle mean and standard deviation of [Envisat-Jason-1] differences of SSH at 10-day dual crossover using the ECMWF wet troposphere correction are plotted in the following figure:

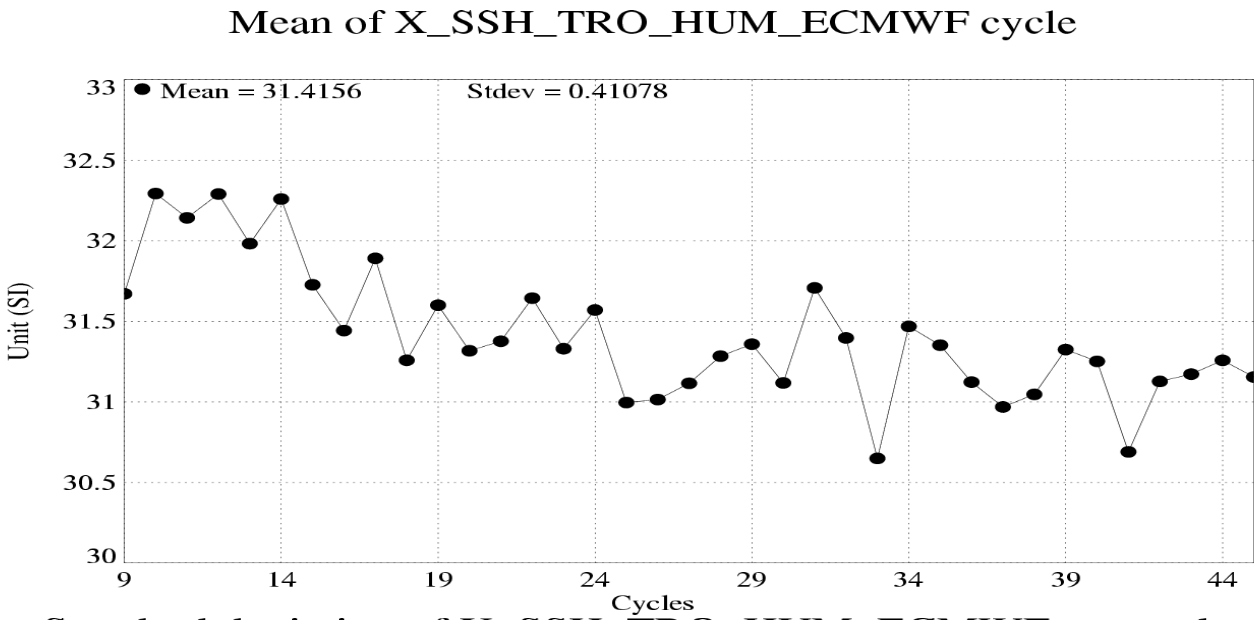

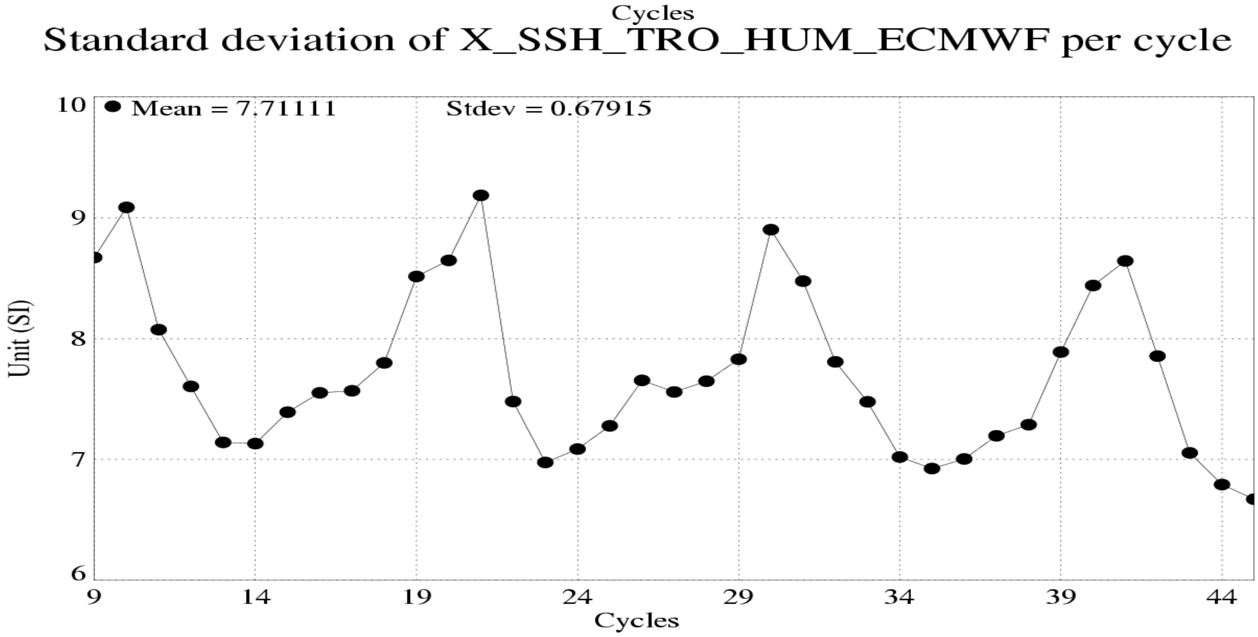

The mean difference decreases during the first year of Envisat (cycles 10-20). Then, the difference stabilizes around 31 cm on cycle 20 onwards. The standard deviation of the difference is reduced on cycle 41 due to the new ground segment configuration.

4.2 SLA Comparisons

Envisat and Jason-1 Sea Level anomalies relative to CLS01 Mean Sea Surface are computed. Global statistics are computed over deep ocean areas (1000 m) and low variability. In order to see fine features, maps are centered about the mean value.

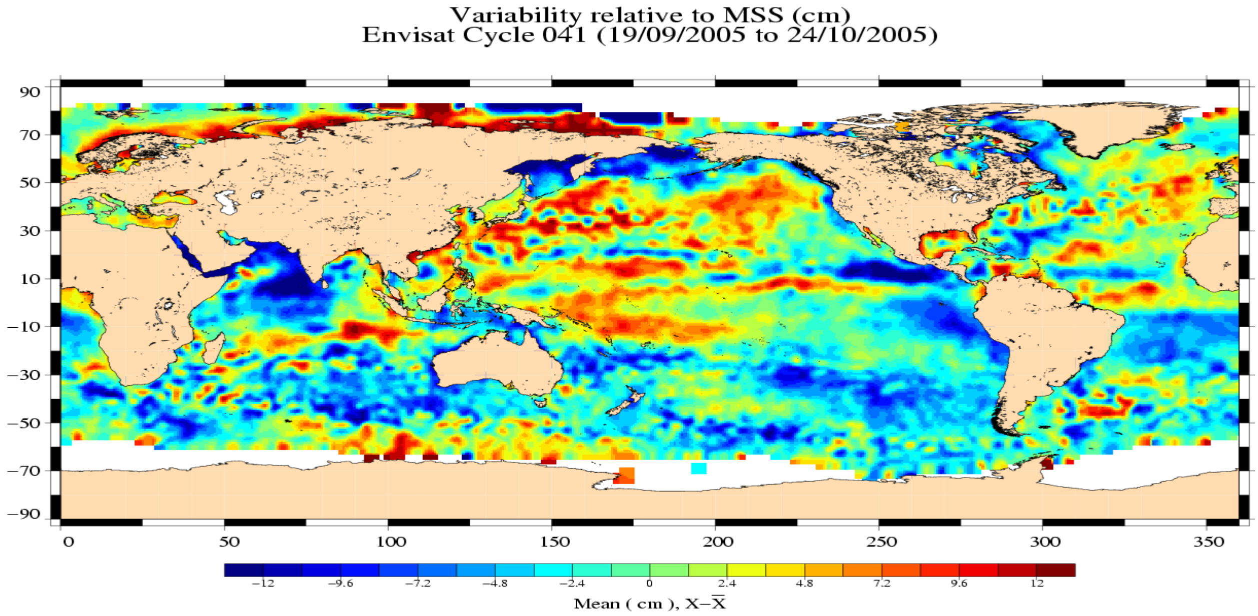

Analysis	Number	Mean (cm)	Std. dev. (cm)
Envisat SLA	1125024	49.12	8.99

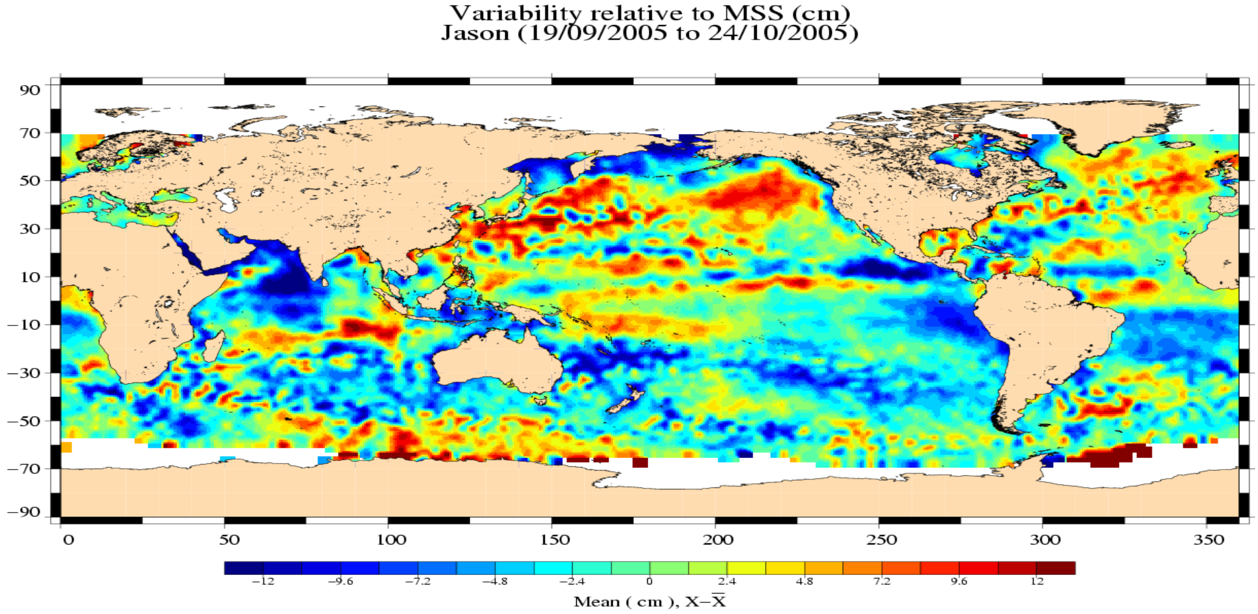

Analysis	Number	Mean (cm)	Std. dev. (cm)
Jason-1 SLA	1202224	18.68	9.30

There is a very good correlation between the two maps. The SLA standard deviation for both

Envisat and Jason-1 is about 9.5 cm. Differences are mainly due to the spatial and temporal sampling of the ocean.

4.3 Long wavelength error reduction

4.3.1 Long wavelength error

The Envisat long wavelentgth error has been computed by global minimization of (EN-J1) SSH differences. The method is described in (Le Traon et al., 1998 [7]). The map of the error is plotted on the following figure (data are centered about the mean value):

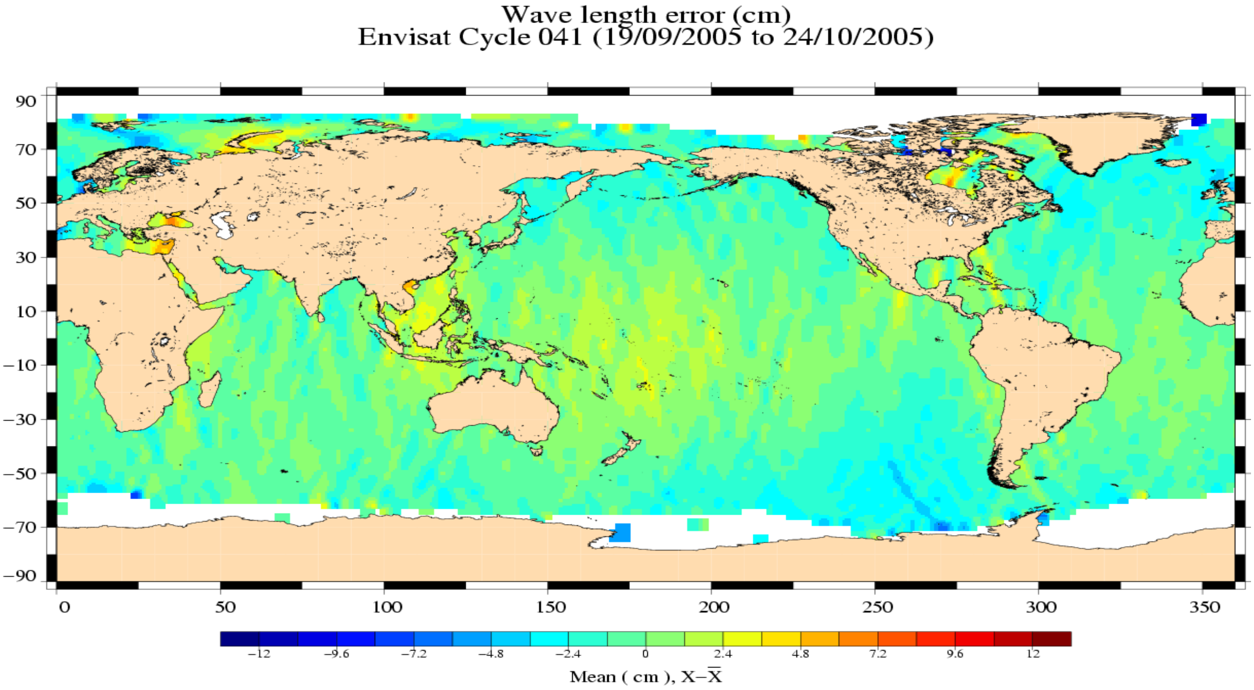

Analysis	Number	Mean (cm)	Std. dev. (cm)
Envisat lw error	1330127	30.60	2.57

The estimated long wavelength error has a small variance which confims the good quality of the Envisat orbit.

4.3.2 Impact on crossover performances

Global statistics for 35 days [Envisat - Envisat] and 10 days [Envisat - Jason-1] are only computed over deep ocean areas (1000 m) :

Analysis	Number	Mean (cm)	Std. dev. (cm)
EN/EN SSH	33249	-0.16	8.11
EN/EN SSH with orbit error	33249	-0.18	7.73

Analysis	Number	Mean (cm)	Std. dev. (cm)
EN-J1 SSH	69752	30.03	6.84
EN-J1 SSH with orbit error	69752	-0.01	6.53

The [Envisat - Jason-1] difference corrected for the estimate Envisat long wavelength error are plotted on the following figure (data are centered about the mean value):

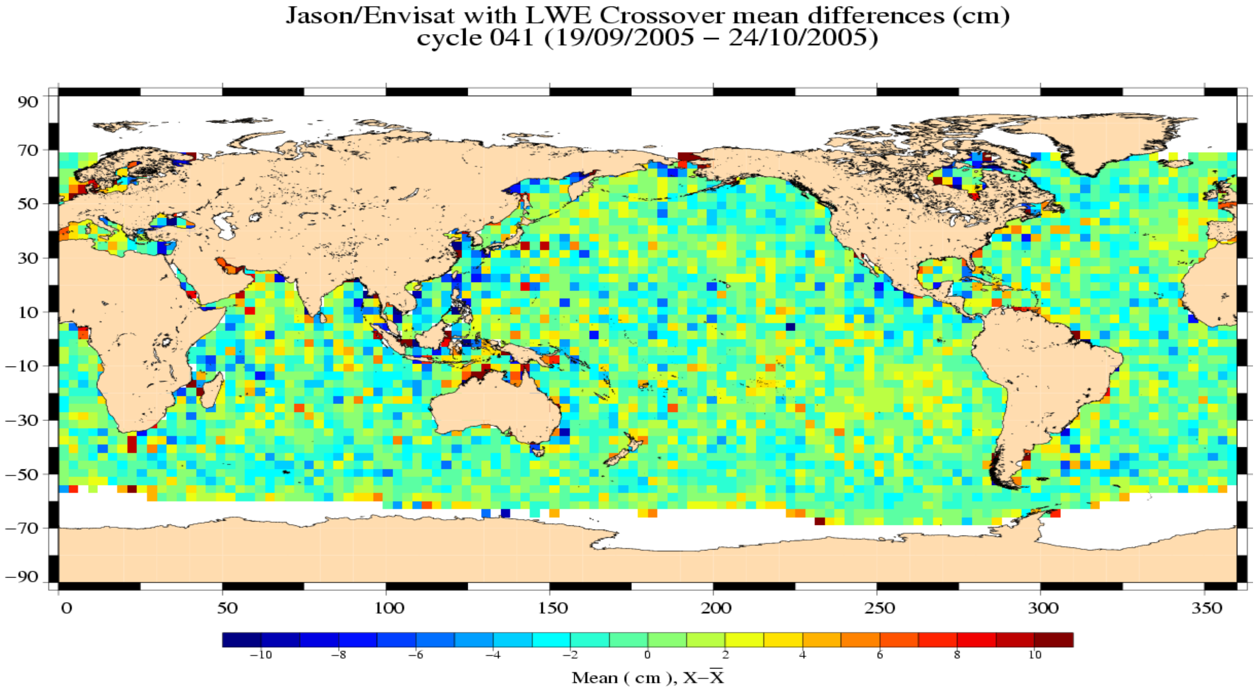

The large scale differences in the Pacific ocean are noticeably reduced.

4.3.3 Impact on SLA performance

Envisat Sea Level anomalies relative to CLS01 Mean Sea Surface using the long wavelength error are computed. Global statistics are computed using a selection to remove shallow waters (1000 m). Map is centered about the mean value.

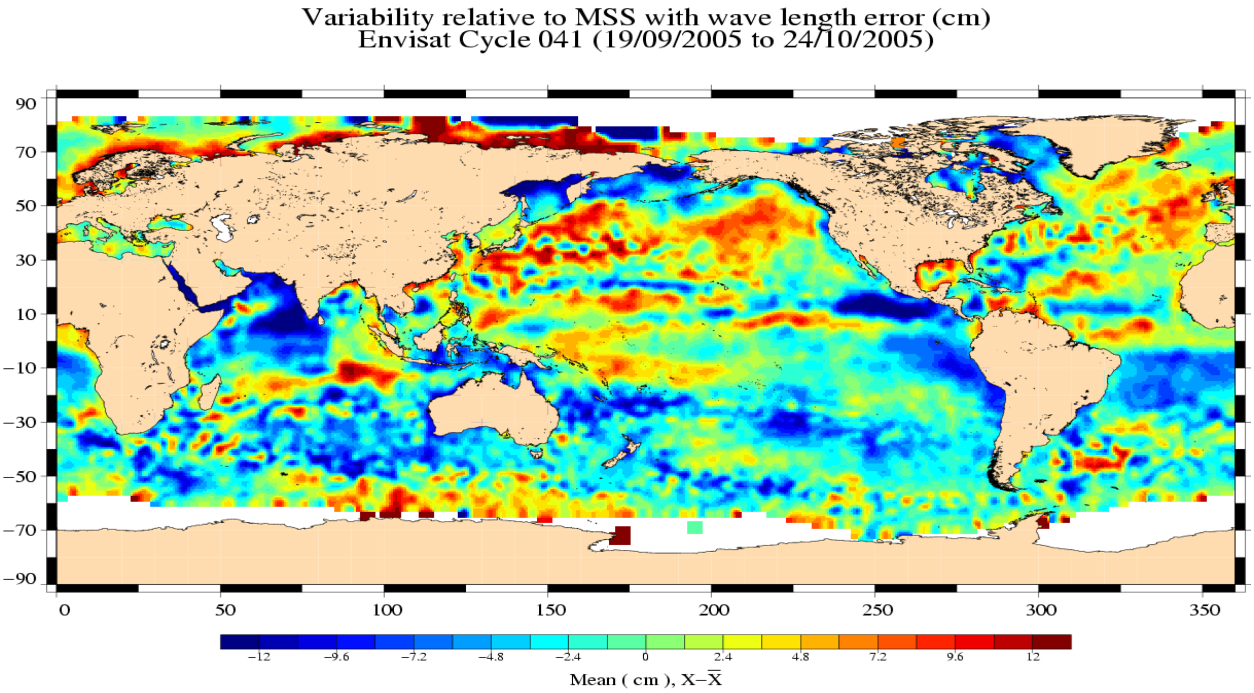

Analysis	Number	Mean (cm)	Std. dev. (cm)
Envisat SLA	1125024	18.53	8.91

The slight impact on Envisat SLA variance shows that the Envisat long wavelength error is low.

4.4 Comparison on a same time/space sampling

Envisat and Jason-1 are now compared on a same time/space sampling:
- 35 day period
- |latitude| < 66

4.4.1 Rms of Ku-band range statistics

The histograms of Envisat and Jason-1 Rms of Ku-band range are given on the following figures:

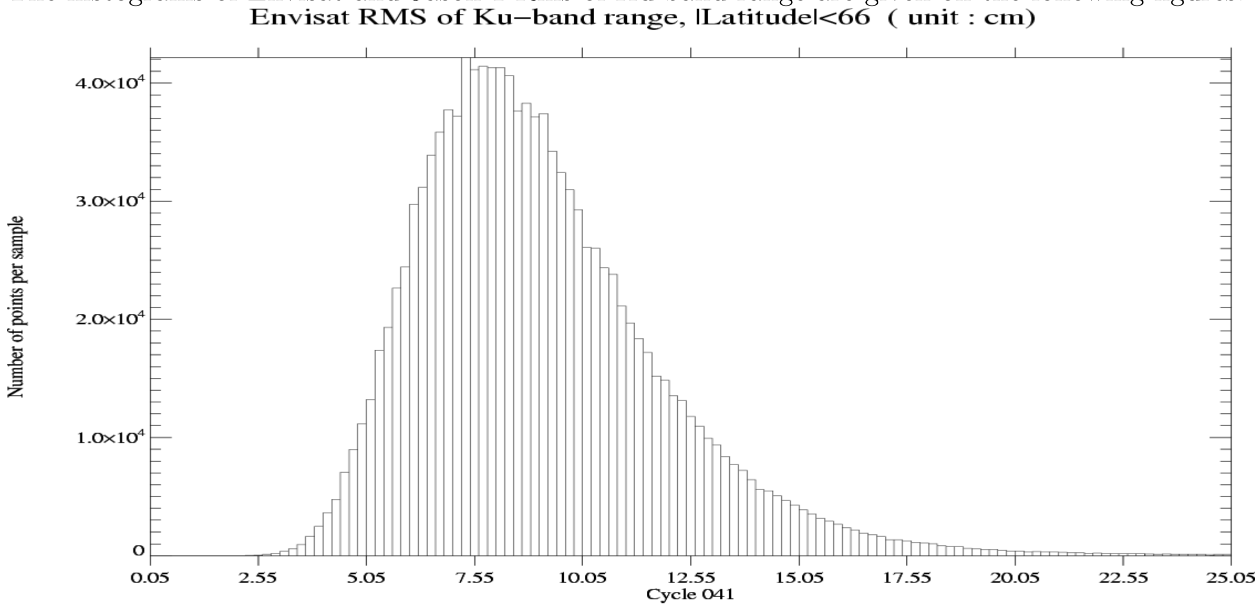

Global nb of points :	1243496	Sel. nb of points	:	1243496	Sample interval :		0.200
Global mean :	9.053	Selected mean	:	9.053	Maximum value :		25.000
Global Std :	2.814	Selected std	:	2.814	Minimum value :		1.600

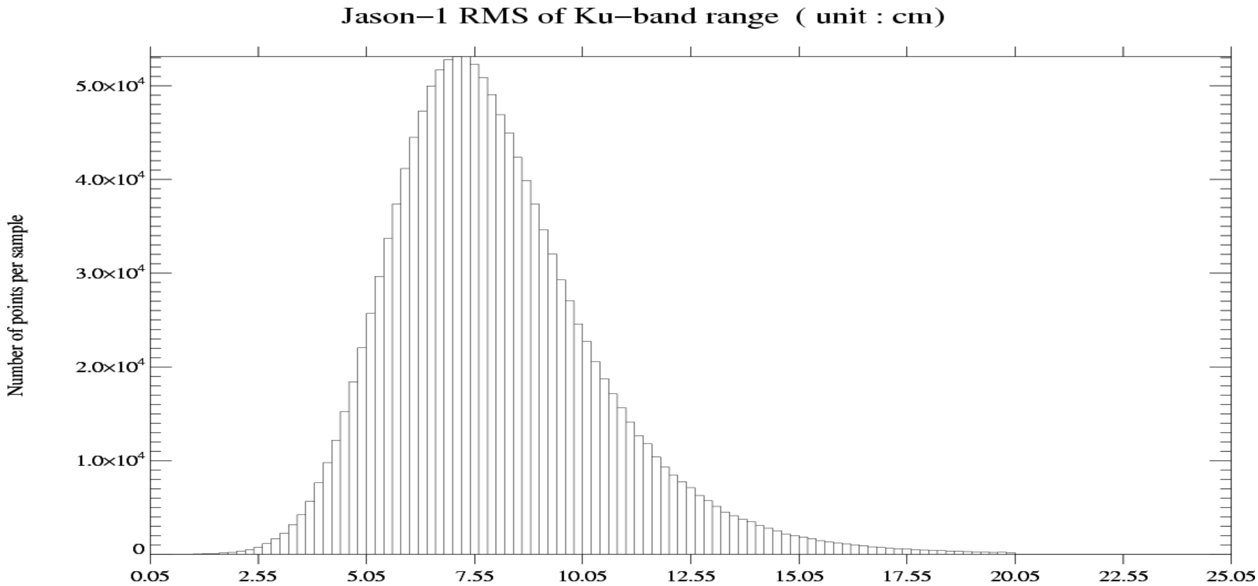

Global nb of points :	1375529	Sel. nb of points	:	1375529	Sample interval :		0.200
Global mean :	8.020	Selected mean	:	8.020	Maximum value :		20.000
Global Std :	2.407	Selected std	:	2.407	Minimum value :		0.900

4.4.2 Ku-band SWH statistics

The histograms of Envisat and Jason-1 Ku-band SWH are given on the following figures:

Envisat Ku−band Significant Wave Height, |Latitude|<66 (unit : m)

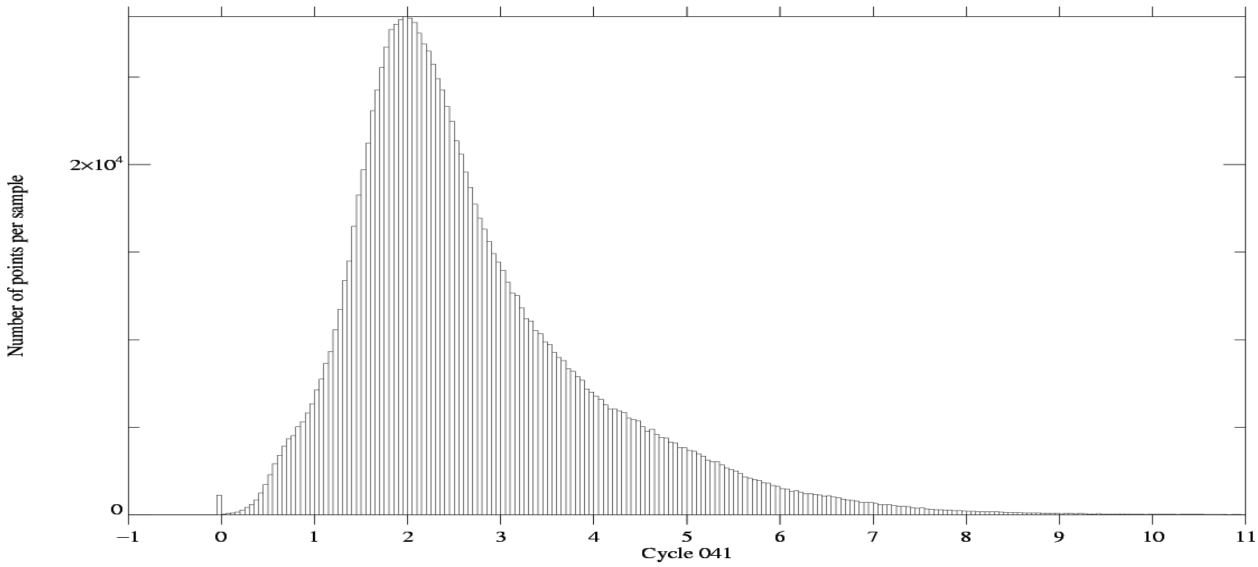

Global nb of points :	1243496	Sel. nb of points :	1243496	Sample interval :	0.050
Global mean :	2.695	Selected mean :	2.695	Maximum value :	10.983
Global Std :	1.321	Selected std :	1.321	Minimum value :	0.000

Jason−1 Ku−band Significant Wave Height (unit : m)

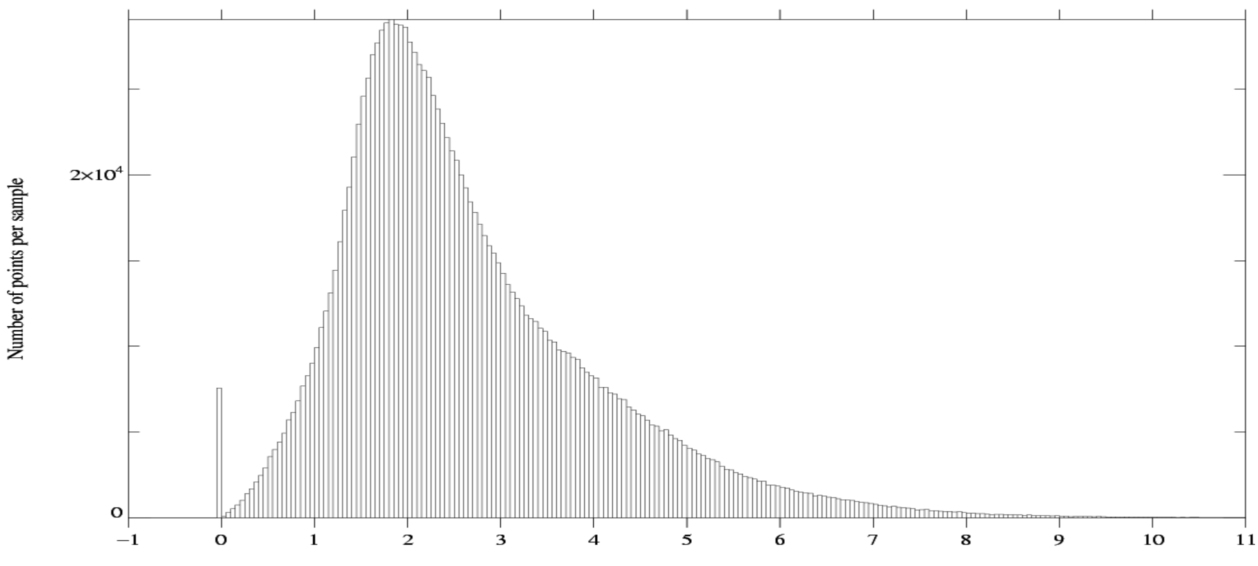

Global nb of points :	1375529	Sel. nb of points :	1375529	Sample interval :	0.050
Global mean :	2.656	Selected mean :	2.656	Maximum value :	10.999
Global Std :	1.397	Selected std :	1.397	Minimum value :	0.000

The cycle per cycle mean of Ku-band SWH measurements for Envisat and Jason-1 is plotted as a fonction of the cycle number on the following figure:

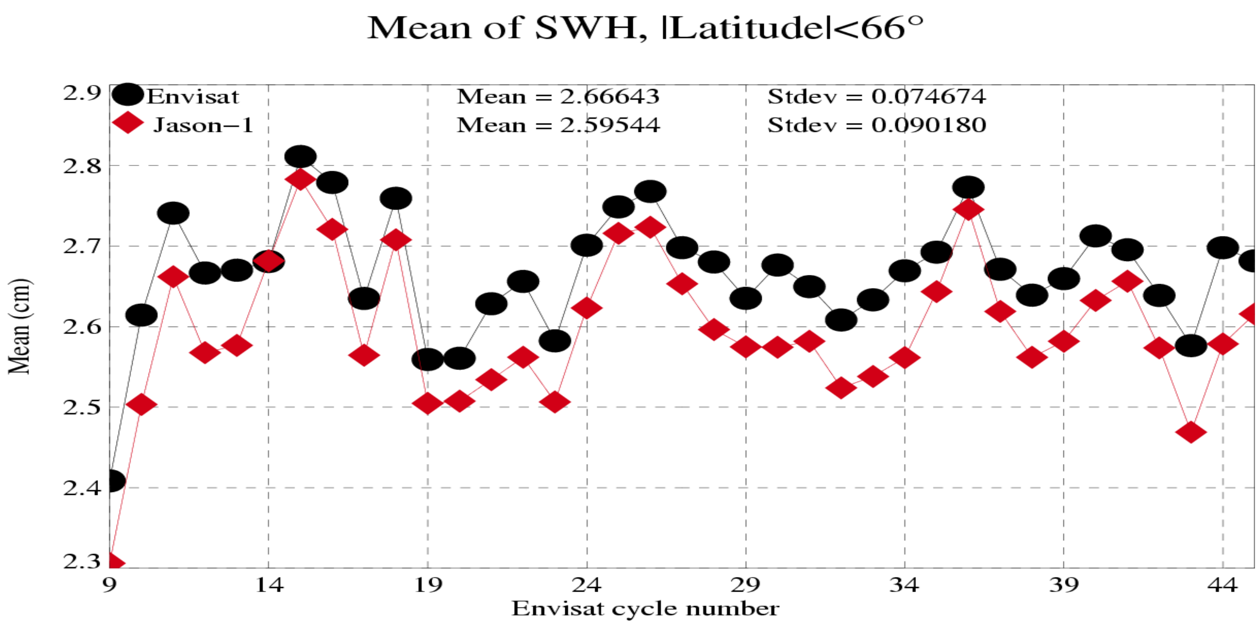

The cycle per cycle mean difference of Ku-band SWH measurements between Envisat and Jason-1 is plotted as a fonction of the cycle number on the following figure:

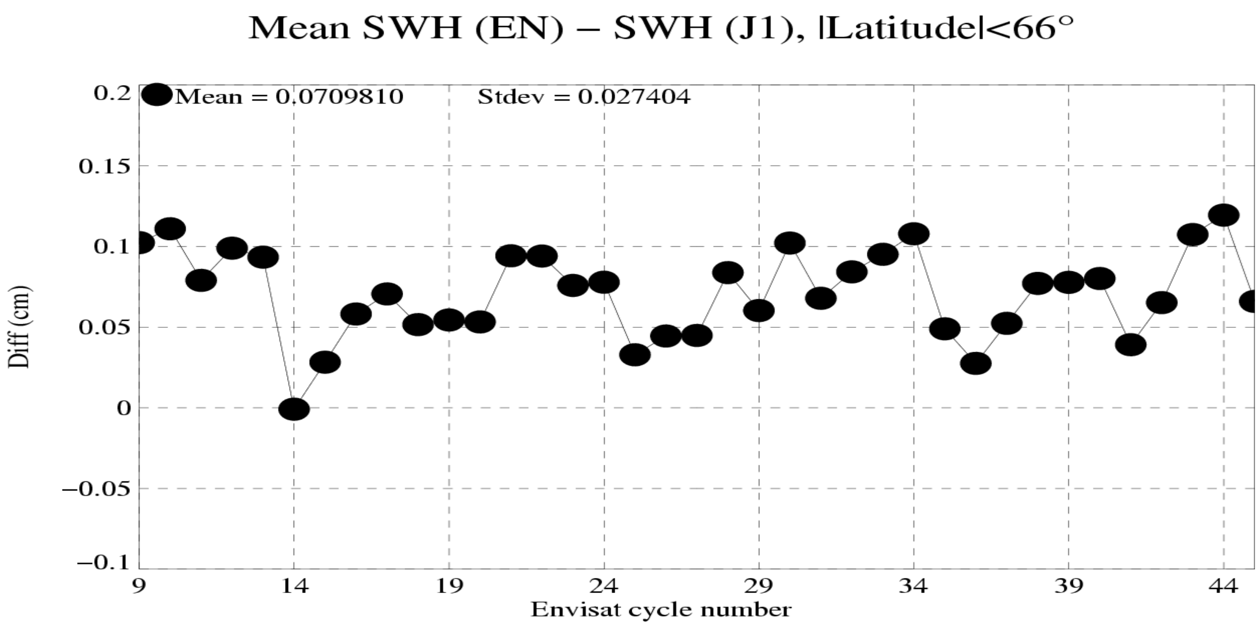

4.4.3 Ku-band Sigma0 statistics

The histograms of Ku-band Sigma0 for Envisat and Jason-1 are given on the following figures:

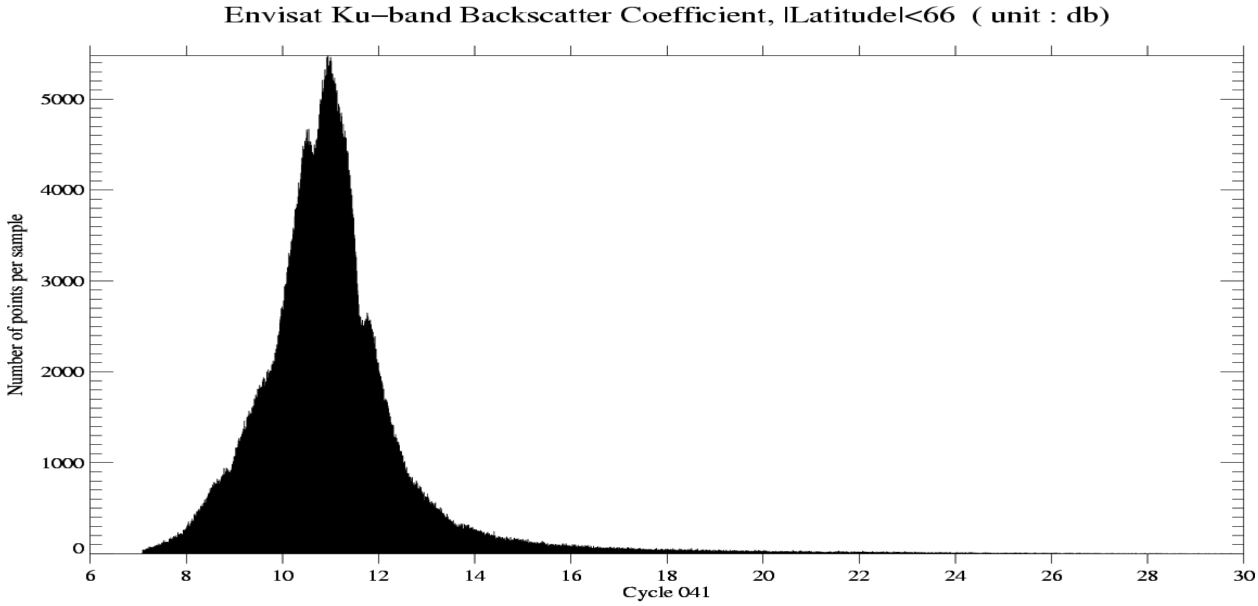

Global nb of points	:	1243496	Sel. nb of points	:	1243496	Sample interval	:	0.010
Global mean	:	11.067	Selected mean	:	11.067	Maximum value	:	29.860
Global Std	:	1.782	Selected std	:	1.782	Minimum value	:	7.080

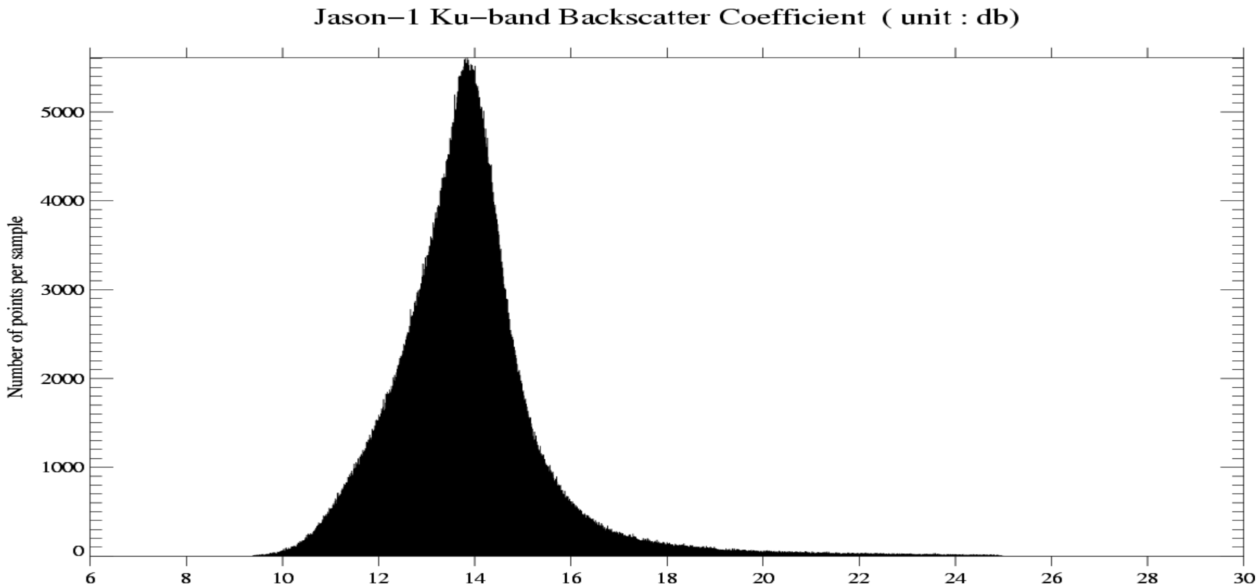

Global nb of points	:	1375529	Sel. nb of points	:	1375529	Sample interval	:	0.010
Global mean	:	13.833	Selected mean	:	13.833	Maximum value	:	25.010
Global Std	:	1.592	Selected std	:	1.592	Minimum value	:	9.380

The general shape of the Envisat histogram is not significantly different from the one obtained at global scale.

The cycle per cycle mean of Ku-band Sigma0 measurements for Envisat and Jason-1 is plotted as a fonction of the cycle number on the following figure:

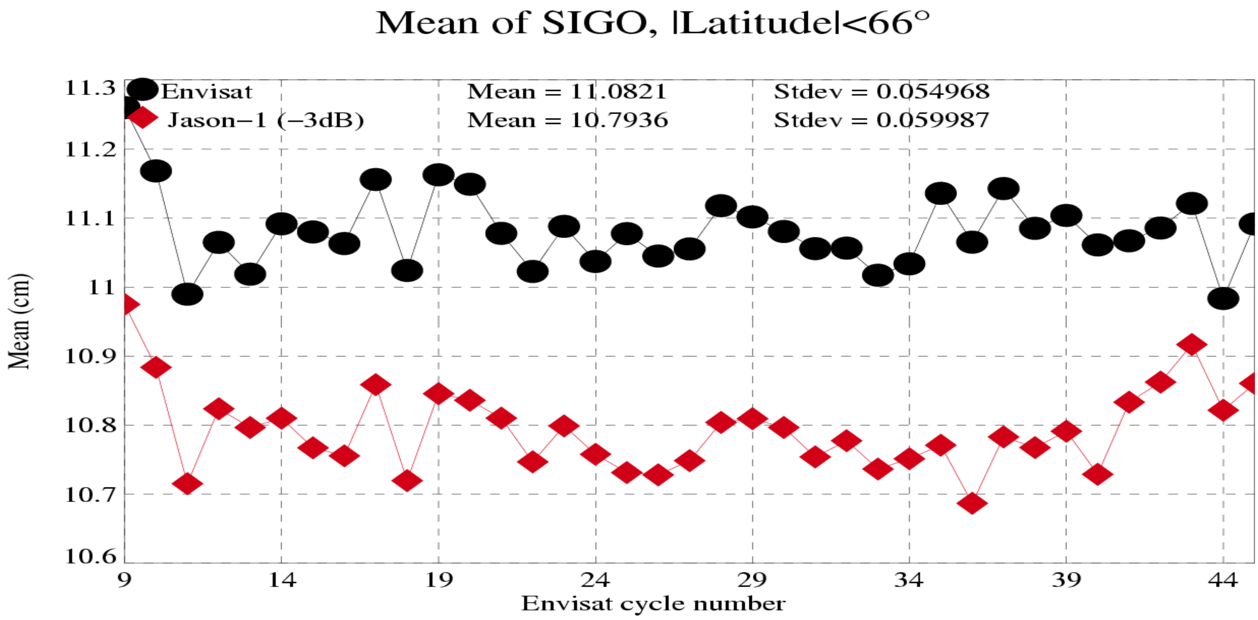

The cycle per cycle mean difference of Ku-band Sigma0 measurements between Envisat and Jason-1 is plotted as a fonction of the cycle number on the following figure:

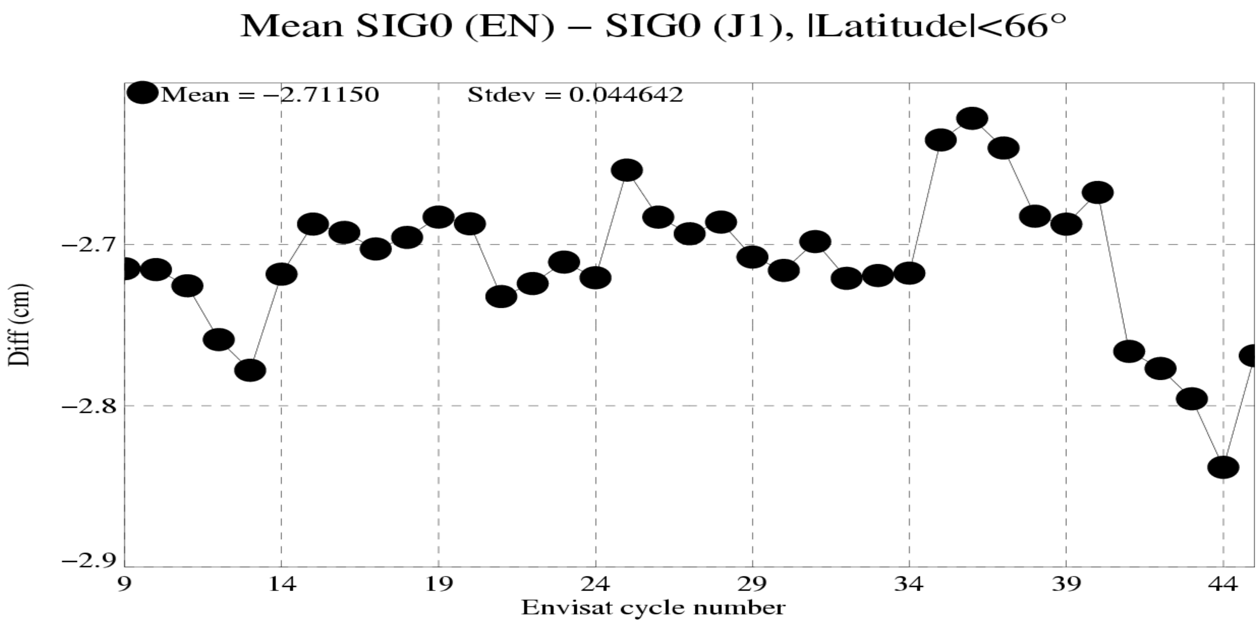

4.4.4 Troposphere statistics

The histograms of Envisat and Jason-1 radiometer wet troposphere correction are given on the following figures:

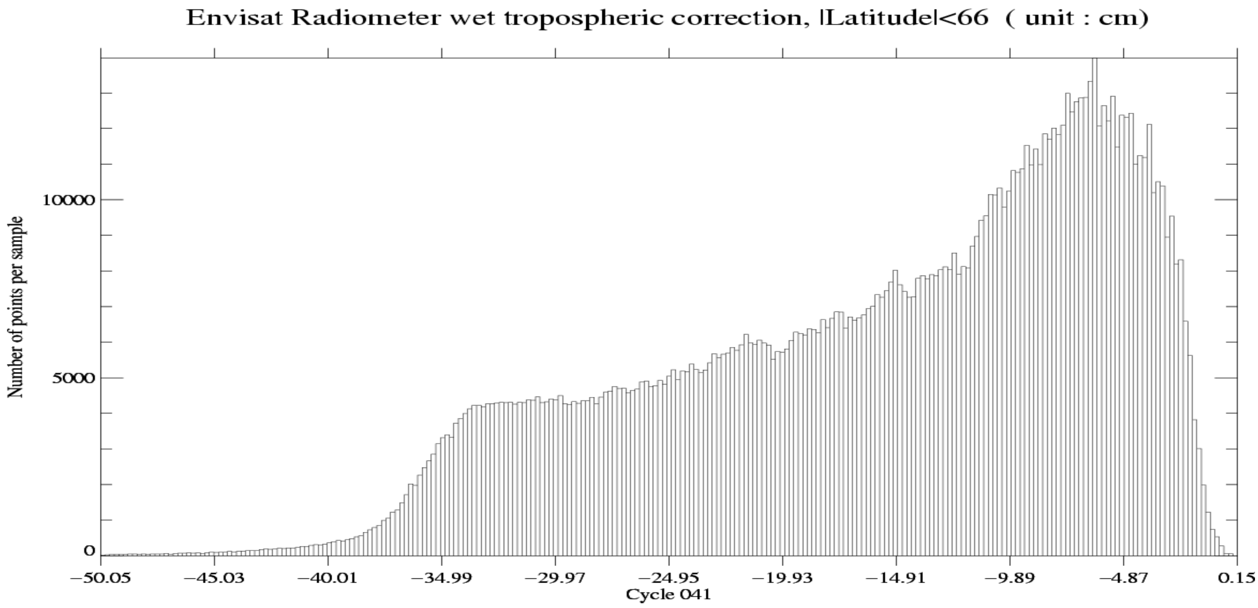

Global nb of points	:	1243496	Sel. nb of points	:	1243496	Sample interval	:	0.200
Global mean	:	−15.603	Selected mean	:	−15.603	Maximum value	:	−0.100
Global Std	:	9.871	Selected std	:	9.871	Minimum value	:	−50.000

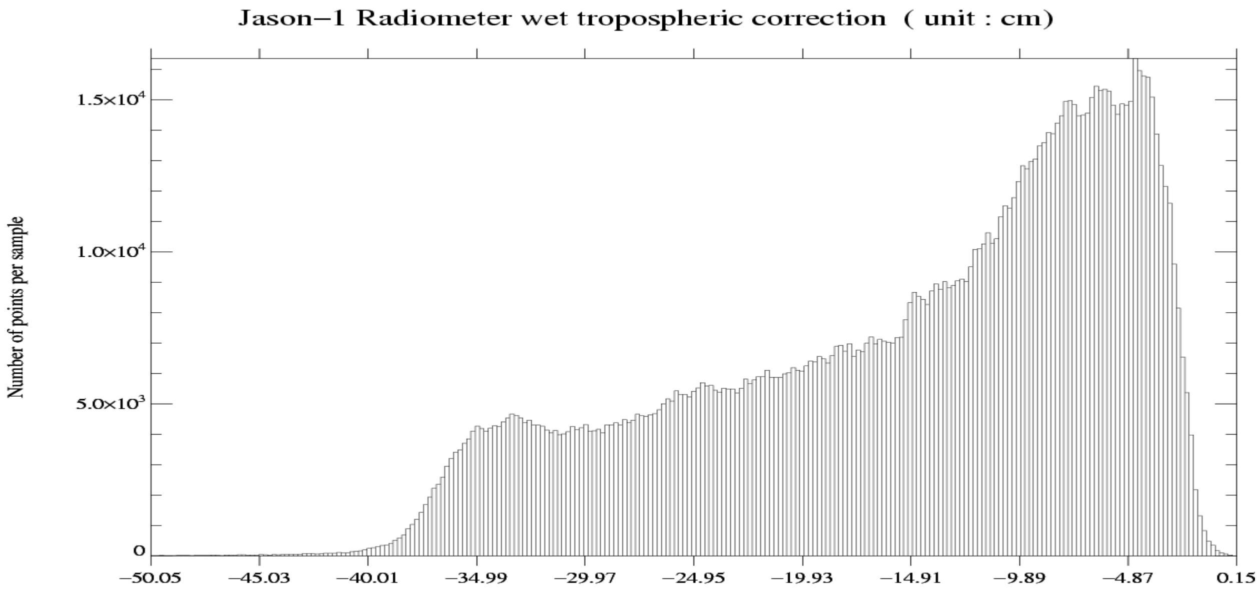

Global nb of points	:	1375529	Sel. nb of points	:	1375529	Sample interval	:	0.200
Global mean	:	−15.183	Selected mean	:	−15.183	Maximum value	:	−0.100
Global Std	:	9.785	Selected std	:	9.785	Minimum value	:	−50.000

4.4.5 SSH crossover performances

10-day crossover points are computed for both Jason-1 and Envisat. Global statistics of SSH differences at crossovers are computed using a selection to remove shallow waters (1000 m):

Analysis	Number	Mean (cm)	Std. dev. (cm)
EN/EN SSH	14816	0.04	6.50

Analysis	Number	Mean (cm)	Std. dev. (cm)
J1/J1 SSH	13298	-0.94	6.89

Using an additional selection to remove areas of high ocean variability and high latitudes (> 50 deg) leads to:

Analysis	Number	Mean (cm)	Std. dev. (cm)
EN/EN SSH	10190	-0.04	5.76

Analysis	Number	Mean (cm)	Std. dev. (cm)
J1/J1 SSH	6998	-0.77	6.19

The cycle per cycle standard deviation of SSH measurements is plotted as a fonction of the cycle number on the following figure:

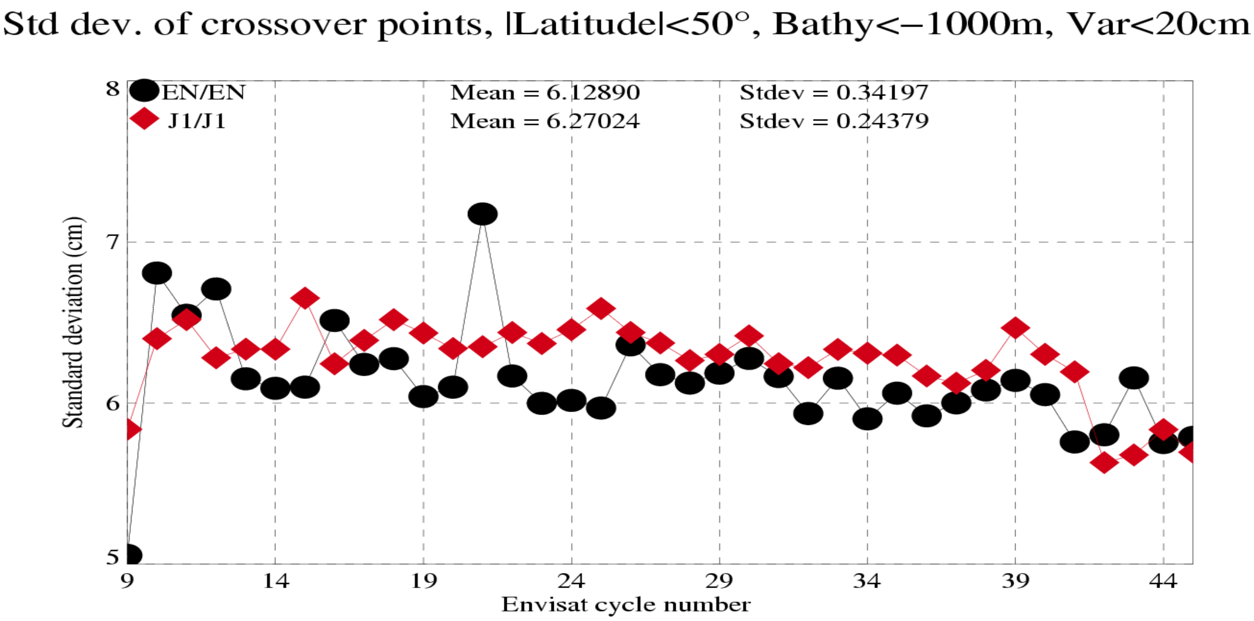

These results show comparable performances for Envisat and Jason-1.

4.4.6 SLA relative to MSS

Envisat and Jason-1 Sea Level anomalies relative to CLS01 Mean Sea Surface are computed. Global statistics are computed removing shallow waters (1000 m) and areas of high ocean variability (20 cm).

Analysis	Number	Mean (cm)	Std. dev. (cm)
Envisat SLA	1135889	49.18	10.05

Analysis	Number	Mean (cm)	Std. dev. (cm)
Jason-1 SLA	1202224	18.68	9.30

These results show comparable performances in terms of SLA variability (standard deviation), and also confirm the crossover estimation of the (Envisat-Jason-1) bias.

References

[1] Ablain M. et al.: Jason-1 GDR quality assessment report, Cycle 136 to 140. *Technical note ALP-RP-P2-EX-21072-CLS* Available at http://www.aviso.oceanobs.com/html/donnees/calval/validation_report/j1/welcome_uk.html

[2] Dorandeu J., 2000: Note on ERS-2 Sigma0 variations since January 2000. *Technical note CLS/DOS/NT/00.286*

[3] EOO/EOX, October 2005, Information to the Users regarding the Envisat RA2/MWR IPF version 5.02 and CMA 7.1 Available at http://earth.esa.int/pcs/envisat/ra2/articles/

[4] Faugere Y. et al.: Envisat GDR quality assessement report (cyclic), Cycle 041, *Technical note SALP-RP-P2-EX-21121-CLS041* Available at http://www.aviso.oceanobs.com/html/donnees/calval/validation_report/en/welcome_uk.html

[5] Gaspar P. and F. Ogor, 1996: Estimation and analysis of the sea state bias of the new ERS-1 and ERS-2 altimetric data (version6). *Report of task 2 of IFREMER Contract N 96/2.246 002/C.*

[6] Labroue S. and E. Obligis, 2003: Neural network retrieval algorithms for the ENVISAT/MWR. *Technical note CLS.DOS/NT/03.848*

[7] Le Traon,P.-Y., F. Ogor, 1998: ERS-1/2 orbit improvement using TOPEX/POSEIDON: The 2cm challenge. *Journal of Geophys. Res., COL. 103, NO. C4, pages 8045-8057*

[8] Martini A., and P. Fmnias, 2000: The ERS SPTR2000 altimetric range correction: Resultats and validation. *ERE-TN-ADQ-GSO-6001*

[9] Martini A., 2003: Envisat RA-2 Range instrumental correction : USO clock period variation and associated auxiliary file, Technical Note ENVI-GSEG-EOPG-TN-03-0009 Available at http://earth.esa.int/pcs/envisat/ra2/articles/USO_clock_corr_aux_file.pdf

[10] Mertz F. et al.: Validation of ERS-2 OPR Cycle 109. *Technical note CLS.OC.NT/03.702 issue 109* Available at http://www.ifremer.fr/cersat/en/documentation/references/oprmon.htm

[11] Obligis E., L. Eymard, N. Tran, 2003: ERS-2/MWR drift evaluation and correction. *Technical note CLS.DOS/NT/03.688*

[12] Picot N., October 21, 2005: New Jason-1 operational production chain. *Electronic communication.*

[13] Scharroo R. and P. N. A. M. Visser, 1998: Precise orbit determination and gravity field improvement for the ERS satellites. *J. Geophys. Res., 103, C4, 8113-8127*

[14] Vincent,P., Desai S.D., Picot N. and Case K., 2003: The first generation of IGDRs and GDRs products to be made available after completion of the Jason-1 verification phase. *Memo to Jason-1 PIs and CoIs.*